

particularly germane to the large number of complexes that contain terminal and bridging sulfides. This conversion represents the second pathway elucidated for the intramolecular assembly of $\mu\text{-}\eta^2\text{-S}_2$ ligands, the first being rotation of a $\mu\text{-}\eta^1\text{-S}_2$ ligand in response to electron deficiency at the metal centers.^{3,29} These arrangements are induced by substrate binding. Similar cooperativity may be anticipated for other metal sulfides.

Acknowledgment. This research was supported by the National Science Foundation (NSF CHE 81-06781). C.M.B. acknowledges fellowships provided by the University of Illinois. The 360-MHz NMR spectra were obtained at the NSF Midwest Regional NMR

facility (NSF 79-16100). Platinum was provided by Engelhardt Industries.

Appendix

See Tables IV and V for positional and thermal parameters for 5.

Registry No. 1, 87174-39-8; 2, 92641-95-7; 3, 92641-96-8; 4, 92641-97-9; 5, 92641-98-0; 6, 92641-99-1; PTD, 4233-33-4; $(\text{CH}_3\text{C}_3\text{H}_4)_2\text{V}_2\text{S}_5$, 82978-84-5; $\text{Pt}(\text{Ph}_3)_2\text{C}_2\text{H}_4$, 12120-15-9; phenylurazole, 15988-11-1.

Supplementary Material Available: Complete lists of distances and angles and calculated and observed structure factor amplitudes (33 pages). Ordering information is given on any current masthead page.

Enhanced Base Hydrolysis of Coordinated Phosphate Esters: The Reactivity of an Unusual Cobalt(III) Amine Dimer

David R. Jones,^{1a} Leonard F. Lindoy,^{*1a} and Alan M. Sargeson^{*1b}

Contribution from the Department of Chemistry and Biochemistry, James Cook University of North Queensland, QLD. 4811 Australia, and Research School of Chemistry, Australian National University, Canberra, A.C.T. 2600, Australia. Received April 16, 1984

Abstract: The hydrolysis of the dimeric cation bis(μ -4-nitrophenyl phosphato)bis[bis(1,2-ethanediamine)cobalt(III)](2+) has been studied at pH 10 and over the hydroxide concentration range 0.05–1.0 M. Product distribution, kinetics (involving 4-nitrophenol release), and ³¹P NMR and ¹⁸O tracer studies were carried out to establish the course of the reaction. In a rapid first step, the eight-membered ring of the dimer is opened by rupture of one of the Co–O bonds (S_N1cB) to give a cis hydroxo complex. The ring-opened species reacts further via two competing pathways: (a) intramolecular attack of the coordinated hydroxide upon the bridging phosphate ester moiety and (b) further cleavage of the dimer by base-catalyzed (S_N1cB) rupture of some Co–O bonds. Route a results in ester hydrolysis with the concomitant formation of a chelated bridging phosphate species whereas route b yields *cis*- and *trans*-hydroxy(*p*-nitrophenyl phosphate)bis(1,2-ethanediamine)cobalt(III). The phosphate chelate ring in the initial product of path a is subsequently opened by Co–O bond rupture and the resultant dimeric bridging phosphato species slowly decomposes to *cis*- and *trans*-hydroxy(phosphato)bis(1,2-ethanediamine)cobalt(III). Comparison of the rate data for hydrolysis of the dimer and the *cis*-hydroxy(4-nitrophenyl phosphato)bis(1,2-ethanediamine)cobalt(III) ion indicates that the attack by the intramolecular nucleophile is largely responsible for the enhanced rate of ester hydrolysis ($\sim 10^5$) with a smaller contribution from charge neutralization at the P center by the metal ion ($\sim 10\text{--}10^2$). Parallel kinetic studies on the analogous dimer bis(μ -4-nitrophenyl phosphato)bis[bis(1,3-propanediamine)cobalt(III)](2+), previously incorrectly formulated as a monomeric species containing chelated phosphate ester, indicate that ester hydrolysis in this complex proceeds by a similar mechanism to that for the 1,2-ethanediamine complex. In total, the results are rationalized in relation to a possible mechanism for the Zn²⁺ containing enzyme E. coli alkaline phosphatase.

Most of the enzymes responsible for the metabolism of phosphate compounds require divalent metal ions such as Mn, Zn, or Mg for activation.² The most studied of these enzymes (the alkaline phosphatase³ and nucleotide kinases⁴) have been shown to have the metal ion present in the active site during the catalytic cycle. However, the precise roles of these ions in the mechanism of catalysis are still far from clear and they need to be displayed in reactive model systems where the route can be defined.

In previous studies, we have investigated the role of metal ions in phosphate ester hydrolysis using structurally well-characterized model compounds and have demonstrated that the hydroxide⁵ and

amido (NH_2^-)⁶ ions coordinated to cobalt(III) are efficient intramolecular nucleophiles for cleaving 4-nitrophenol from coordinated 4-nitrophenyl phosphate. Rate enhancements of 10^5 and 10^8 , respectively, relative to the uncoordinated ester were obtained for these (mononuclear) complexes. There is evidence that the coordination of a phosphate ester simultaneously to two metal ions will also lead to a considerable increase in the rate of ester hydrolysis. For example, the rate of hydrolysis of ATP is enhanced 60–300-fold⁷ in the presence of Cu(II) and this has been attributed to the formation of the dimeric chelate, $[(\text{ATP})\text{Cu}(\text{OH})]_2^{6-}$. Binuclear complexes have been implicated as the reactive entities that are responsible for the increased rates of hydrolysis of ATP in the presence of the lanthanide ions⁸ and $[\text{Co}(1,3\text{-propanedi-$

(1) (a) James Cook University. (b) Australian National University.

(2) Dixon, M.; Webb, E. C. "Enzymes", 2nd ed.; Longman, Green and Co.: New York, 1971; pp 422–424. Morrison, J. F.; Heyde, E. *Annu. Rev. Biochem.* **1972**, *41*, 29.

(3) Reid, T. W.; Wilson, I. B. "The Enzymes", 3rd ed.; Boyer, P. D., Ed.; Academic Press: New York, 1971; Vol. 4, pp 373–409.

(4) (a) Watts, D. C. "The Enzymes", 3rd ed.; Boyer, P. D., Ed.; Academic Press: New York, 1973; Vol. 8A, pp 384–431. (b) Morrison, J. F. ref 4a, 1973; Vol. 8, pp 475–485. (c) Mildvan, A. S. ref 4a, 1973; Vol. 2, pp 499–501.

(5) Jones, D. R.; Lindoy, L. F.; Sargeson, A. M. *J. Am. Chem. Soc.* **1983**, *105*, 7327.

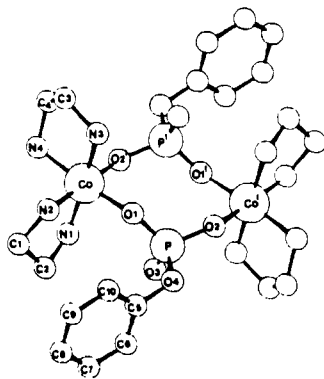
(6) Harrowfield, J. MacB; Jones, D. R.; Lindoy, L. F.; Sargeson, A. M. *J. Am. Chem. Soc.* **1980**, *102*, 7733.

(7) Spiro, T. G.; Kjellstrom, W. A.; Zydel, M. C.; Butow, R. A. *Biochemistry* **1968**, *7*, 859. Sigel, H.; Hofstetter, F. *Eur. J. Biochem.* **1983**, *132*, 569.

amine)₂(OH)₂(OH)]²⁺.⁹ In the latter case there is a 10⁵-fold increase in rate relative to uncoordinated ATP at pH 7. The rate of hydrolysis of triphosphate in solutions of β,γ-[Co(NH₃)₄H₂P₃O₁₀] is increased also by 10⁴ times when [Co(cyclen)(H₂O)₂]³⁺ is added.¹⁰ This enhancement has been attributed to the formation of a binuclear complex, followed by intramolecular hydrolysis of the phosphate chain by a coordinated hydroxide ion.

Circumstantial evidence for the dimeric structure of the CuATP complex is provided by the crystal structures of ternary metal-amine-mononucleotide complexes in which the phosphate moieties of two mononucleotide molecules bridge two metal atoms,¹¹ resulting in a puckered eight-membered ring. Recently, bis-[(adenosine 5'-triphosphate)(2,2'-bipyridine)zinc(II)] tetrahydrate has also been shown by X-ray diffraction to be dimer, with two zinc atoms held together by two OPO bridges from the γ-phosphate groups of two ATP moieties.¹² However, it has not been determined whether these dimeric structures persist in solution.

We have recently reported the synthesis and X-ray structure of the bis[(μ-phenyl phosphato)bis(1,2-ethanediamine)cobalt(III)] cation (1) in which an eight-membered ring is defined by two



1

cobalt atoms and the bridging phosphate groups of the two ester moieties.¹³ The dimeric solution has been shown to persist in aqueous solution and the base hydrolysis of this complex and of its 4-nitrophenyl analogue are discussed in this paper.

The base hydrolysis of 4-nitrophenyl phosphate in a complex that was formulated as [Co(tn)₂O₃POC₆H₄NO₂]₂ClO₄ (tn = 1,3-propanediamine) has been described previously.¹⁴ The phosphate ester was proposed to coordinate via a four-membered chelate ring with the attendant strain leading to rapid hydrolysis of the ester in base to yield free nitrophenolate ions. The evidence for bidentate coordination was adduced largely from the anhydrous nature of the isolated complex, the consequent absence of a deprotonatable coordinated water molecule and the rapidity of the process (10⁹-fold greater than the uncoordinated ester). The mechanism of base hydrolysis was proposed to involve intermolecular attack of hydroxide ion at the phosphorus center to yield a less stained bidentate pentaoxyphosphorane intermediate. Rapid decay of this intermediate to phosphate and nitrophenolate ion was argued to lead to complexes containing phosphate, but the lability of the Co(tn)₂ system prevented their characterization. The advent of routine ³¹P NMR spectroscopy in our laboratories and a crystal structure of the analogous 1,2-ethanediamine system mentioned above, coupled with conductivity and molecular weight measurements, have now shown that the formulation of the tn complex as a monomer was incorrect.¹⁵ The structure and re-

action path of this complex has now been reanalyzed in the light of the new facts described above.

Experimental Section

¹H NMR spectra were recorded by using a JEOL JNM-MH-100 (MINIMAR) spectrometer. All shifts are quoted as parts per million downfield relative to DSS [sodium 3-(trimethylsilyl)propanesulfonate]. ³¹P{H} NMR spectra were recorded by using a Bruker B-KR spectrometer operating at 24.281 MHz with external D₂O as a field frequency lock. For the kinetic studies, a JEOL JNM-FX-100 (³¹P probe) or a JEOL JNM-FX-90 (multi probe) spectrometer operating at 40.32 and 36.20 MHz, respectively, with internal D₂O lock were used. ³¹P chemical shifts are reported relative to external 85% H₃PO₄. ¹³C{H} NMR spectra were recorded by using a JEOL FX-60Q spectrometer (chemical shifts are relative to 1,4-dioxane).

An autobalancing resistance bridge (Genrad 1657 RLC Digibridge) was used in conjunction with a Philips PW 9512/00 electrode for the conductance measurements. A Knauer Dampfdruck-Osmometer was used for the determination of molecular weights in aqueous solution.

Electronic spectra and rate data were obtained with a Cary 118C spectrophotometer. Molar absorptivities are quoted in units of M⁻¹ cm⁻¹. All evaporations were carried out by using a Büchi rotary evaporator under reduced pressure (τ < 20 mmHg) so that the temperature of the solution did not exceed 15 °C.

Analytical grade reagents were used throughout except where otherwise specified. Dimethyl sulfoxide (Mallinkrodt, AR) was dried over 4A molecular sieves. Laboratory reagent grade sulfolane (tetramethylene-sulfone) was predried by passage through a column of 4A molecular sieves and then distilled from calcium hydride immediately before use. Nitronium tetrafluoroborate (NO₂BF₄) was obtained from Pfaltz and Bauer Inc.

The synthesis of [[Co(en)₂(μ-O₃POC₆H₅)₂]₂(CF₃SO₃)₂·2H₂O and the isolation of the *racemic* and *meso* diastereoisomers have been reported previously.¹³ A mixture of *meso* and *racemic* [Co(tn)₂(μ-O₃POC₆H₄NO₂)₂]²⁺ was obtained by using the previously published procedure.¹² Authentic samples of [Co(en)₂PO₄] and [Co(en)₂(OH₂)(PO₄H)]ClO₄ were synthesized by published procedures.¹⁶ [Co(en)₂(OH₂)(O₃POC₆H₄NO₂)]ClO₄ was prepared as previously described.³

Nitration of *meso*- and *rac*-[[Co(en)₂(μ-O₃POC₆H₅)₂]₂(CF₃SO₃)₂·2H₂O. The nitration procedure was the same for each of the diastereoisomers. All manipulations involving the nitronium tetrafluoroborate were carried out under a dry nitrogen atmosphere in a glovebag. The complex (2 g) was placed in a 50-mL conical flask (containing a stirrer bar) that had previously been purged with dry N₂. Anhydrous sulfolane (16 mL) and the solid complex were dispersed by vigorous agitation. The reaction was initiated by the addition of NO₂BF₄ (0.9 g). The flask was sealed and removed from the glovebag. The reaction mixture was then stirred vigorously and the starting material dissolved rapidly to produce a deep red solution. The reaction was quenched after 12 min by slowly pouring the solution into a vigorously stirred ether/ethanol mixture (4:1 v/v, 1 L); stirring was continued for 25 min and the product was obtained as a viscous gum. Trituration of the gum in absolute ethanol (70 mL) converted it into a pink powder. Ether (130 mL) was then slowly added with stirring, and the suspension was stirred for 15 min. The pale pink powder was collected by filtration and washed with ether (yield 1.5 g). The recrystallization procedures differ for the two diastereoisomers since the perchlorate salt of the *rac* form is much more soluble than that of the *meso* form.

Meso Diastereoisomer. The crude product was dissolved in a minimum volume of water by stirring the solid with a slurry of AG1-X8 (Cl⁻ form) resin. The resin was removed and the volume of the filtrate adjusted to 30 mL by the addition of water and methanol (3 mL). Dropwise addition of an aqueous solution of NaClO₄ (30 mL of 1.6 M) to the stirred filtrate resulted in the crystallization of the complex. The pink-violet microcrystalline product was collected, washed with ice-cold 3 M NaClO₄ (5 mL), ice-cold methanol (6 mL), and ether (10 mL), and finally dried in vacuo over P₂O₅ for 18 h. Anal. Calcd for [[Co(C₂H₈N₂)₂(μ-O₃POC₆H₄NO₂)₂](ClO₄)₂·H₂O: C, 23.80; H, 4.19; N, 13.87; P, 6.14; Co, 11.68. Found: C, 23.9; H, 4.0; N, 13.5; P, 6.9; Co 11.4. The ¹H NMR spectrum of a saturated solution of the chloride salt of the complex in 1 mL of D₂O containing 12 M DCl (0.04 g) gave the following chemical shifts (δ, relative peak areas and multiplicities in parentheses): CH₂, 2.50 (4, br); CH₂, 2.90 (4, br); NH₂, 4.44 (4, br); NH₂, 5.88 (4, br); aromatic H, 7.28 (2, d), 8.18 (2, d). The ¹³C NMR

(8) Selwyn, M. J. *Nature (London)* **1968**, *219*, 490.

(9) Hediger, M.; Milburn, R. M. *J. Inorg. Biochem.* **1982**, *16*, 165.

(10) Norman, P. R.; Cornelius, R. D. *J. Am. Chem. Soc.* **1982**, *104*, 2356.

(11) Fischer, B. E.; Bau, R. *Inorg. Chem.* **1978**, *17*, 27. Ya Wei, C.; Fishcher, B. E.; Bau, R. *J. Chem. Soc., Chem. Commun.* **1978**, 1053.

(12) Oriolo, P.; Cini, R.; Donati, D.; Mangani, S. *J. Am. Chem. Soc.* **1981**, *103*, 4446. Cini, R.; Oriolo, P. *J. Inorg. Biochem.* **1981**, *14*, 95.

(13) Jones, D. R.; Lindoy, L. F.; Sargeson, A. M.; Snow, M. R. *Inorg. Chem.* **1982**, *21*, 4155.

(14) Anderson, B.; Milburn, R. M.; Harrowfield, J. MacB.; Robertson, G.; Sargeson, A. M. *J. Am. Chem. Soc.* **1977**, *99*, 2652.

(15) Our suspicions about the original interpretation were aroused by the appearance of three ³¹P NMR signals in the analogous "[Co(en)₂O₃POC₆H₅]₂SO₃CF₃" complex that was subsequently shown to be dimeric and to exist as *meso* and *racemic* isomers (see ref 13).

(16) Lincoln, S. F.; Stranks, D. R. *Aust. J. Chem.* **1968**, *21*, 37.

assignments (δ) are as follows: CH₂, -20.96 (s); CH₂, -23.34 (s); aromatic C₁, 91.32 (d, $^2J_{\text{POC}} = 6.6$ Hz); C_{2,6}, 54.69 (d, $^3J_{\text{POCC}} = 4.4$ Hz); C_{3,5}, 59.18 (s); C₄, 76.88 (s). ^{31}P NMR: 13.33 ppm (s) in water. Visible spectrum: $\epsilon_{510}^{\text{max}} = 207$ in water. When NaCF₃SO₃ was substituted for NaClO₄ in the recrystallization procedure, the complex was isolated as its triflate salt. Anal. Calcd for $\{[\text{Co}(\text{C}_2\text{H}_5\text{N}_2)_2(\mu\text{-O}_3\text{POC}_6\text{H}_4\text{NO}_2)]_2(\text{CF}_3\text{SO}_3)_2\}$: C, 24.23; H, 3.70; N, 12.85; P, 5.68; Co, 10.81; F, 10.45. Found: C, 24.0; H, 3.6; N, 12.8; P, 5.9; Co, 10.5; F, 10.6.

Racemic Diastereoisomer. The crude product was treated as before with anion-exchange resin. The solution was filtered and the resin washed with water (5 mL). The combined filtrate and washings were diluted to 25 mL. Dropwise addition of 4 M NaClO₄ (25 mL) to the stirred solution resulted in the formation of pink-violet microcrystals. The solution was kept at 0 °C for 1 h. The product was then collected, washed with ice-cold 4 M NaClO₄ (5 mL), ether/methanol mixture (5:1 v/v, 5 mL), and ether, and finally dried in vacuo over P₂O₅ for 18 h. Anal. Calcd for $\{[\text{Co}(\text{C}_2\text{H}_5\text{N}_2)_2(\mu\text{-O}_3\text{POC}_6\text{H}_4\text{NO}_2)]_2(\text{ClO}_4)_2 \cdot 2\text{H}_2\text{O}\}$: C, 23.38; H, 4.32; N, 13.63; Co, 11.48. Found: C, 23.6; H, 4.5; N, 13.9; Co, 11.2. The ^1H NMR spectrum of a saturated solution of the chloride salt of the complex in 1 mL of D₂O containing 12 M DCl (0.04 g) gave the following chemical shifts (δ , relative peak areas and multiplicities in parentheses): CH₂, 2.50 (4, br); CH₂, 2.90 (4, br); NH₂, 4.44 (4, br); NH₂, 5.88 (4, br); aromatic H, 7.28 (2, d), 8.18 (2, d). The ^{13}C NMR assignments are as follows: CH₂, -21.05; CH₂, -21.27 (s); CH₂, -22.91 (s); aromatic C₁, two sets of overlapping doublets at 91.20 (d, $J_{\text{POC}} = 6.6$ Hz) and 91.54 (d, $J_{\text{POC}} = 6.6$ Hz); C_{2,6}, two sets of overlapping doublets at 53.93 (d, $^3J_{\text{POCC}} = 5.1$ Hz) and 54.10 (d, $^3J_{\text{POCC}} = 5.1$ Hz); C_{3,5}, 59.21 (s), C₄, 76.75 (s). ^{31}P NMR: two peaks at 13.16 and 13.35 ppm in D₂O. Visible spectrum: $\epsilon_{510}^{\text{max}} = 214$ in water.

The rac diastereoisomer was resolved into its chiral forms by the same procedure as that used for the resolution of the *rac*-bis(μ -phenyl phosphate) dimer.¹³ The data for the (-)_D enantiomer are given. Anal. Calcd for (-)_D- $\{[\text{Co}(\text{C}_2\text{H}_5\text{N}_2)_2(\mu\text{-O}_3\text{POC}_6\text{H}_4\text{NO}_2)]_2(\text{ClO}_4)_2 \cdot \text{H}_2\text{O}\}$: C, 23.81; H, 4.20; N, 13.89. Found: C, 23.9; H, 4.2; N, 13.7 ($[\text{M}]_{589} = -1167$; $[\text{M}]_{545}^{\text{min}} = -3389$; $[\text{M}]_{463}^{\text{max}} = +3111$ deg mol⁻¹ m⁻¹ in water at 25 °C).

Spectrophotometric Kinetics. The release of 4-nitrophenol from *meso*- and *rac*- $\{[\text{Co}(\text{en})_2(\mu\text{-O}_3\text{POC}_6\text{H}_4\text{NO}_2)]_2\}^{2+}$ was followed spectrophotometrically (400 nm) at pH 10 and over the hydroxide concentration range 0.05–1.0 M. For the measurement of rates in the hydroxide solutions, a hand-operated stopped-flow mixer was used. The release of nitrophenol is a three-step process. The steps are as follows: (i) an induction period during which no nitrophenol is released, (ii) rapid release of nitrophenol, and (iii) slow release of nitrophenol. The rate constant for the third step was obtained by analyzing the data obtained from the absorbance–time trace after the second step was complete. The rate for the second step was obtained by using an extrapolated initial velocity plot for the third reaction.¹⁷ This method effectively subtracts the absorbance resulting from the third reaction from the total absorbance and enables the evaluation of the rate constant by plotting the log ($A_{\infty} - A_t$) data against time. The resultant plot was initially curved due to the induction period. The curved section was discarded, and the required rate constant was calculated from the slope of the linear segment.

Some information about the product distribution for the hydrolysis reaction can also be obtained from the kinetics. The value of A_{∞}^1 extrapolated to A_0^1 represents the total nitrophenol released during the rapid second step. Since the total amount of nitrophenol initially present in the starting material is known (T), the percentage of nitrophenol produced by the second step can be evaluated. Subtraction of A_0^1 from the total absorbance change (A_{∞}) allows the yield of nitrophenol produced by the third step to be calculated. The percentage yield of nitrophenol (Y) from the base hydrolysis of *cis*- $[\text{Co}(\text{en})_2(\text{OH})_2\text{O}_3\text{POC}_6\text{H}_4\text{NO}_2]^+$ is known⁵ (this is the product that is responsible for nitrophenol release in the slow third step), and thus the effective total yield of this complex can be determined:

$$\text{cis-}[\text{Co}(\text{en})_2(\text{OH})_2\text{O}_3\text{POC}_6\text{H}_4\text{NO}_2] = \frac{100(A_{\infty} - A_0^1)}{Y(18700)} \frac{V}{1000} \frac{100}{T} \%$$

The terms ($A_{\infty} - A_0^1$), T , and Y have been defined above, 18700¹² is the molar absorptivity of the 4-nitrophenolate anion at 400 nm, and the factor $V/1000$ is required to convert molar concentration to moles.

Product Distribution. *rac*- $\{[\text{Co}(\text{en})_2(\mu\text{-O}_3\text{POC}_6\text{H}_4\text{NO}_2)]_2\}\text{Cl}_2$ (0.25 g) was dissolved in water (25 mL) at 25 °C. The base hydrolysis was

initiated by the rapid addition with stirring of 3 M NaOH solution (5 mL). The reaction was quenched after $4t_{1/2}$ (for the rapid nitrophenol-releasing step) by the addition of 2 M HClO₄ until the pH of the solution was ca. 3.8. The solution was then diluted to 2 L with ice-cold water and sorbed rapidly under pressure on Sephadex C-25 resin (Na⁺ form, 16 × 3 cm; column flow rate ~35 mL/min) that had been washed immediately beforehand with ice-cold water (300 mL at pH 3.8 with 0.005 M acetate buffer). The initial effluent containing the free nitrophenol and nitrophenyl phosphate was collected, and the column was then washed with cold water until the effluent no longer turned yellow when made alkaline. The initial effluents and washings were combined and analyzed for nitrophenol and total nitrophenol as described previously.⁶ Elution of the cationic species with 0.1 M NaClO₄ (pH 4) revealed the presence of five bands. The first two (pale blue-violet and red, respectively) were easily removed and corresponded to *trans*- and *cis*- $[\text{Co}(\text{en})_2(\text{OH})_2\text{O}_3\text{POC}_6\text{H}_4\text{NO}_2]^+$, respectively. When these bands had eluted, the eluent was changed to 0.2 M NaClO₄. The third band (red-violet) was then rapidly eluted from the column. The two remaining red-orange fractions were then eluted with 0.4 M NaClO₄. The first of these corresponded to $[\text{Co}(\text{en})_2(\text{OH}_2)]^{3+}$. The identities of the complexes corresponding to the third and fifth bands are discussed later. To facilitate discussion of the product distribution results, the first fraction corresponding to nitrophenol and nitrophenyl phosphate is designated as band 1 and five cationic fractions that were initially adsorbed on the cation-exchange column are designated bands 2–6. All eluates were analyzed for cobalt, nitrophenol, and phosphate by methods described previously⁶ and by atomic absorption spectroscopy.

Kinetics and Product Identification (by ^{31}P NMR Spectroscopy). The base hydrolysis products of the mixed and individual diastereoisomers of $\{[\text{Co}(\text{en})_2(\mu\text{-O}_3\text{POC}_6\text{H}_4\text{NO}_2)]_2\}^{2+}$ were studied under a variety of conditions. Solutions of the complexes were prepared by gently warming (~40 °C) and stirring a suspension of the appropriate perchlorate salt (ca. 55 mg) and Dowex AG1-X8 (Cl⁻ form) resin in water (2.0 mL) containing trimethyl phosphate (0.21 mL of TMP in 100 mL of water) as internal reference [δ (TMP) 3.0 relative to external 85% H₃PO₄]. The resin was filtered, and 1.5 mL of the filtrate was transferred to a 10-mm NMR tube. D₂O (0.3 mL) was added, and the tube was placed in the probe. The temperature of the solution was adjusted to the required value (measured by a thermocouple inserted into the tube) by passing chilled nitrogen gas through the probe assembly. The reaction was then initiated by the rapid addition of 0.2 mL of the appropriate NaOH solution (2 or 10 M) that had been equilibrated to the same temperature as the metal complex solution. An analogous series of experiments was carried out for the complex that was formulated originally as $[\text{Co}(\text{tn})_2\text{O}_3\text{POC}_6\text{H}_4\text{NO}_2]\text{ClO}_4$.¹⁴

Thirteen spectra were accumulated for the hydrolysis of the *meso* diastereoisomer in 0.2 M hydroxide solution at 5 (± 1) °C. The peak heights of all spectra were normalized relative to the height of the trimethyl phosphate internal reference peak in spectrum 2 so that the relative amounts of each product could be plotted as a function of time. Accumulation of the first spectrum was started 60 s after the addition of base. Each spectrum was accumulated for 100 s, with a 15-s delay between spectra (required for transfer of the data to magnetic tape). The midpoint in the spectral accumulation was therefore taken as the "time" for each spectrum. The peak height for spectrum 1 was plotted at 110 s and that for spectrum 2 at 225 s (160 + 15 + 50 s) and so on. The spectral parameters for all of the experiments described in the figures are as follows: frequency, 40.3 MHz; bandwidth, 2100 Hz; pulse angle, 60°; pulse rate, 1 s; 100 transients/spectrum.

The base hydrolysis of *meso*- $\{[\text{Co}(\text{en})_2(\mu\text{-O}_3\text{POC}_6\text{H}_4\text{NO}_2)]_2\}^{2+}$ was investigated in 0.2 M hydroxide solution at 28 °C. A solution of the complex was prepared by stirring a suspension of the perchlorate salt (50 mg) and Dowex AG1-X8 (Cl⁻ form) resin in water (2 mL). The resin was removed by filtration, and 1.8 mL of the filtrate was transferred to a 10-mm NMR tube. The tube was placed in the probe and the temperature of the solution adjusted as described above. The reaction was initiated by the rapid addition of 2 M NaOH solution (0.2 mL), and spectra were accumulated at 0 s, 910 s, 1790 s, 2670 s, and 18 h after mixing. Spectral parameters: frequency, 24.28 MHz; bandwidth, 2083 Hz; pulse angle, 60 °C; pulse rate, 1 s, external lock. The peak corresponding to the phenyl phosphate product of the reaction was used as an internal reference (δ 0.0 ppm relative to external 85% H₃PO₄).

^{18}O Tracer Experiment. The isolation of nitrophenyl phosphate and nitrophenol from solution and the subsequent procedures for determination of their ^{18}O contents have been described previously.⁶ $\{[\text{Co}(\text{en})_2(\mu\text{-O}_3\text{POC}_6\text{H}_4\text{NO}_2)]_2(\text{CF}_3\text{SO}_3)_2\}$ (0.5 g) was added, with stirring, to 2.93 atom % H₂¹⁸O that was 0.2 or 1.0 M in sodium hydroxide. The reaction was allowed to proceed for $20t_{1/2}$, and then the solvent was removed on a vacuum line. The residue was dissolved in water (1 L) and the pH of the solution adjusted to 4 by the addition of nitric acid. The

(17) Jackson, W. G.; Harrowfield, J. MacB.; Vowles, P. D. *Int. J. Chem. Kinet.* 1977, 9, 535.

(18) Edwards, J. D.; Foong, S. W.; Sykes, A. G. *J. Chem. Soc., Dalton Trans.* 1973, 829.

Table I. Determination of Electrolyte Type by Conductance Measurements^a in Water

complex	electrolyte type	slope
[Co(en) ₂ CO ₃]ClO ₄ ^c	1:1	123
[Co(en) ₂ (glycinate)](ClO ₄) ₂ ^c	1:2	180
<i>meso</i> -[[Co(en) ₂ (μ-O ₃ POC ₆ H ₅) ₂]Cl ₂	1:2	195
<i>rac</i> -[[Co(en) ₂ (μ-O ₃ POC ₆ H ₅) ₂]Cl ₂	1:2	172
<i>meso</i> -[[Co(en) ₂ (μ-O ₃ POC ₆ H ₄ NO ₂) ₂]Cl ₂	1:2	178
[[Co(tn) ₂ (μ-O ₃ POC ₆ H ₅) ₂]Cl ₂ ^d	1:2	192
[[Co(tn) ₂ (μ-O ₃ POC ₆ H ₄ NO ₂) ₂]Cl ₂ ^d	1:2	195
[Co(en) ₃](ClO ₄) ₃ ^c	1:3	333

^aFeltham, R. D.; Hayter, R. G. *J. Chem. Soc.* **1964**, 4587-4591.
^bSlope of $\Delta_0 - \Delta_\infty$ vs. $(c)^{1/2}$ plot (c is the equivalent concentration, equiv dm⁻³). Units are Ω^{-1} cm² equiv⁻¹ dm^{3/2}. Precision $\pm 6\%$. The mean slope for 1:2 electrolytes is 185 ± 11 . ^cElectrolyte standards. ^dMixed diastereoisomers.

Table II. Determination of Molecular Weights by Vapor Pressure Osmometry in Water

complex	mol wt	
	calcd	found ^a
<i>meso</i> -[[Co(en) ₂ (μ-O ₃ POC ₆ H ₅) ₂]Cl	791	843
<i>rac</i> -[[Co(en) ₂ (μ-O ₃ POC ₆ H ₅) ₂](OAc) ₂ ^b	820	858
<i>meso</i> -[[Co(en) ₂ (μ-O ₃ POC ₆ H ₄ NO ₂) ₂](OAc) ₂	911	971
[[Co(tn) ₂ (μ-O ₃ POC ₆ H ₅) ₂]Cl ₂	884	888
[[Co(tn) ₂ (μ-O ₃ POC ₆ H ₄ NO ₂) ₂](OAc) ₂	966	900
[Co(en) ₂ PO ₄]-2H ₂ O ^c	310	337
[Co(en) ₂ CO ₃]ClO ₄ ^c	339	343
[Co(en) ₂ glycinate](ClO ₄) ₂ ^c	452	489

^aPrecision $\pm 7\%$. ^bOAc is the acetate anion. ^cStandard samples used for controls.

cationic reaction products were removed by passing the solution through a column of Sephadex C25 (Na⁺ form) resin. The effluent from this column was collected, and the nitrophenyl phosphate and nitrophenol that it contained were separated by chromatography on a column of DEAE Sephadex (NO₃⁻ form). The details of the chromatography, the isolation of the products from solution, and the subsequent procedures for determination of their ¹⁸O contents have been described previously.⁶ The ¹⁸O contents of the products for both the 0.2 and 1.0 M OH⁻ hydrolyses were identical (nitrophenol, 0.0% enrichment; nitrophenyl phosphate, 0.0% enrichment).

Results

Synthesis. The *meso* and *rac* diastereomers of [[Co(en)₂(μ-O₃POC₆H₅)₂](CF₃SO₃)₂ were nitrated in sulfolane with NO₂BF₄ to yield the corresponding diastereoisomers of the bis(*μ-p*-nitrophenyl phosphato) dimer. The integrity of the products was confirmed by the characteristic ³¹P NMR and ¹³C NMR spectra of the two forms. Further evidence for the preservation of the dimeric structure for the cation during nitration was provided by conductivity measurements and molecular weight determinations on the nitration product. The conductance and molecular weight data for this and a range of other cobalt(III) complexes, including [[Co(tn)₂(μ-O₃POC₆H₄NO₂)₂](OAc)₂, are summarized in Tables I and II.

Kinetics (by Spectrophotometry). The release of 4-nitrophenol from the *meso* and *rac* diastereoisomers of the [[Co(en)₂(μ-O₃POC₆H₄NO₂)₂]²⁺ cation was followed spectrophotometrically at pH 10 and over 0.05–1.0 M hydroxide. A typical absorbance vs. time curve is illustrated in Figure 1; it is apparent that the production of nitrophenol is a complex multistep process. There is an initial induction period during which no nitrophenol is produced (Figure 1, inset). This is followed by rapid release of nitrophenol in the second stage of the reaction. Finally, there is a much slower third process that also yields nitrophenol. A simple reaction scheme that accounts for these observations is given by (1) where $k_1 > k_2$ and $k_3, k_2 \approx k_3$, and k_2 and $k_3 \gg k_4$.

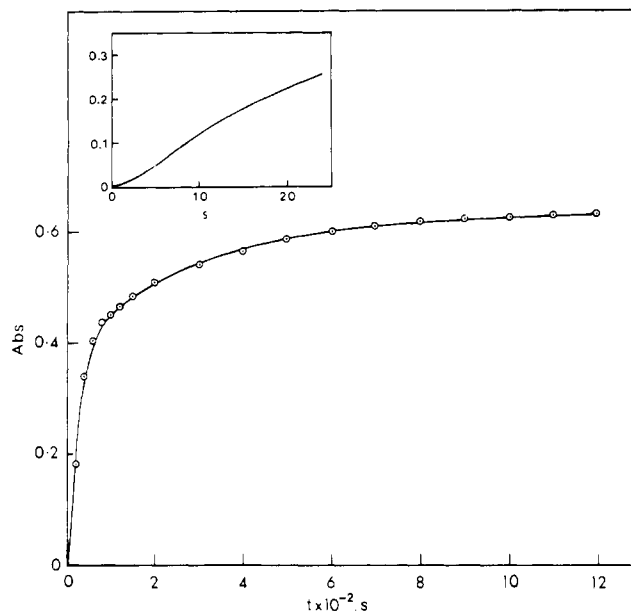
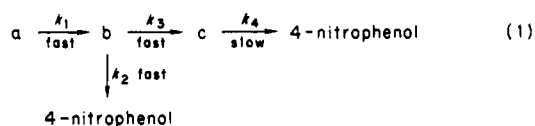


Figure 1. A typical absorbance vs. time curve for the base hydrolysis of *meso*-[[Co(en)₂(μ-O₃POC₆H₄NO₂)₂]²⁺. Conditions: [OH⁻] = 0.5 M; $T = 25^\circ\text{C}$; [complex] = 5×10^{-4} M; wavelength, 400 nm. Inset shows the first 20 s of the reaction.

Table III. Kinetic and Product Distribution Data for the Rapid Nitrophenol-Releasing Step of the Base Hydrolysis of the Diastereoisomers of [[Co(en)₂(μ-O₃POC₆H₄NO₂)₂]²⁺

[OH ⁻], M	<i>meso</i>		<i>racemic</i>	
	$10^2 k_2$, ^a s ⁻¹	yield of NP, ^b %	$10^2 k_2$, ^a s ⁻¹	yield of NP, ^b %
0.05	0.47	31	0.81	30
0.1	1.0	28	1.4	28
0.25	2.1	23	3.0	28
0.5	4.5	16	4.9	16
0.75	7.0	13	7.9	13
1.0	10.5	12	11.8	11

^aEach entry is the average of three values that differed by not more than 4%. ^bPercent yield of nitrophenol (NP) that is equal to $(A_0^1/T) \times 100$; see text for explanation of terms). Accuracy is $\pm 5\%$ of the quoted percentage yield.

The rate of the slow step (k_4) was determined by analyzing the data obtained from the absorbance–time trace after the rapid release of nitrophenol in the second stage of the reaction. The plot of $\log(A_\infty - A_t)$ vs. time was linear for at least $4t_{1/2}$ confirming that the reaction was first order. The values for k_4 over the range of hydroxide concentrations studied were identical with the rate constants obtained for the hydrolysis of *cis*-[Co(en)₂(OH)₂O₃POC₆H₄NO₂]⁺ under the same conditions.⁵ This implied that one of the base hydrolysis products of the dimer was the mononuclear complex *cis*-[Co(en)₂(OH)₂O₃POC₆H₄NO₂]. The rate constants for the rapid nitrophenol-producing step ($k_2 + k_3$) in (1) were obtained by using the procedure described in the Experimental Section. The values are listed in Table III and are plotted against hydroxide concentration in Figure 2. The *racemic* diastereoisomer reacted approximately 1.5 times faster than the *meso* diastereoisomer. Each of the diastereoisomers exhibited a first-order dependence on hydroxide concentration up to 0.5 M ($k_2 = 8.8 \times 10^{-2}$ M⁻¹ s⁻¹ for the *meso* diastereoisomer), but above this a systematic upward-curving deviation from linearity occurs. A similar deviation was observed for the base hydrolysis of *cis*-[Co(en)₂(OH)₂O₃POC₆H₄NO₂].⁵

Information concerning the product distribution can also be obtained from the kinetics. The yield of nitrophenol from the second step of the reaction and the amount of *cis*-[Co(en)₂(OH)₂O₃POC₆H₄NO₂] produced was calculated by using the procedure described in the Experimental Section. The results of this analysis for each of the hydroxide concentrations are listed in

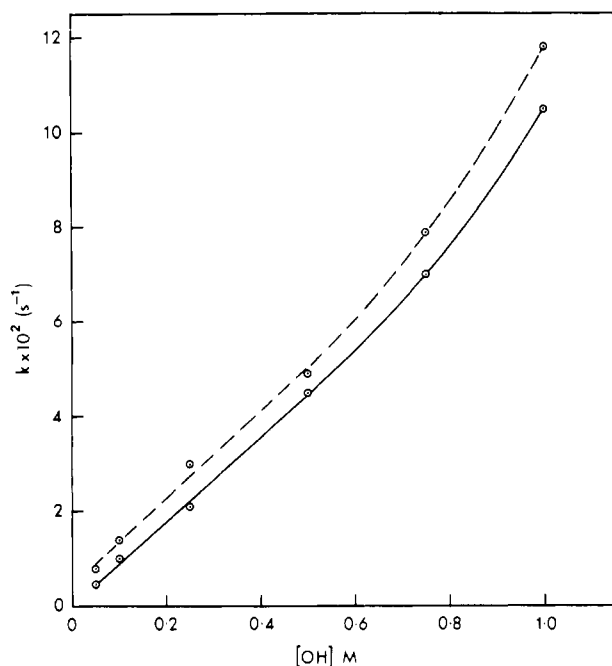


Figure 2. Plot of k_{obsd} vs. $[\text{OH}^-]$ for the rapid nitrophenol-producing step in the base hydrolysis of the meso (—) and racemic (---) diastereoisomers of $[\text{Co}(\text{en})_2(\mu\text{-O}_3\text{POC}_6\text{H}_4\text{NO}_2)_2]^{2+}$ ($T = 25^\circ\text{C}$; $\mu = 1\text{ M NaClO}_4$).

Table IV. Calculated Yield (%) of $\text{cis-}[\text{Co}(\text{en})_2(\text{OH})\text{O}_3\text{POC}_6\text{H}_4\text{NO}_2]$ for the Base Hydrolysis of *meso*- and *rac*- $[\text{Co}(\text{en})_2(\mu\text{-O}_3\text{POC}_6\text{H}_4\text{NO}_2)_2]^{2+}$

$[\text{OH}^-]$, M	<i>cis</i> - $[\text{Co}(\text{en})_2(\text{OH})\text{O}_3\text{POC}_6\text{H}_4\text{NO}_2]$, ^b %	
	<i>meso</i>	<i>racemic</i>
0.05	20	
0.25	28	
0.5	32	33
0.75	38	39
1.0	34	37

^a Calculated from the spectrophotometric kinetic data. ^b Accuracy ± 3 .

Table IV. Although the *rac* diastereoisomer produces nitrophenol at approximately 1.5 times the rate of the *meso* form in the fast second step after the induction period, the data show that the percentage yields of nitrophenol and *cis*- $[\text{Co}(\text{en})_2(\text{OH})\text{O}_3\text{POC}_6\text{H}_4\text{NO}_2]$ are the same for both diastereoisomers. Clearly, a considerable amount of nitrophenol that was present in the starting material is not released in the second and third steps. Quantitative studies were undertaken in order to ascertain the fate of the nitrophenol unaccounted for in the above spectrophotometric experiments.

Product Distribution. Quantitative product distribution studies were carried out in duplicate for the hydrolysis of the racemic diastereoisomer of the bis(μ -nitrophenyl phosphato) dimer at hydroxide concentrations of 0.5 and 1.0 M. The conclusions from these studies can be extended to the *meso* diastereoisomer since the spectrophotometric kinetics have already shown that both diastereoisomers produce the same yields (within experimental error) of nitrophenol and *cis*- $[\text{Co}(\text{en})_2(\text{OH})\text{O}_3\text{POC}_6\text{H}_4\text{NO}_2]$.

The complex was allowed to react for $4t_{1/2}$ (based on the rate of the rapid nitrophenol-releasing step that follows the induction period) before quenching the solution to pH 4. The cationic hydrolysis products were then sorbed on Sephadex C-25 resin at 7°C . Low-temperature conditions were employed in order to minimize the possibility of the cobalt-containing species undergoing post-quench reactions. The neutral and anionic products (nitrophenol and nitrophenyl phosphate, respectively) did not bind to the cation exchange resin and were collected in the column

Table V. Product Distributions for the Base Hydrolysis of $\text{rac-}[\text{Co}(\text{en})_2(\mu\text{-O}_3\text{POC}_6\text{H}_4\text{NO}_2)_2]^{2+}$ ($[\text{OH}^-] = 0.5$ and 1.0 M)

band	$[\text{OH}^-] = 0.5\text{ M}$			$[\text{OH}^-] = 1.0\text{ M}$		
	Co, ^a %	NP, ^{a,b} %	P, ^a %	Co, ^a %	NP, ^{a,b} %	P, ^a %
1 ^c	0	37	17	0	37	25
2	23	23	23	27	27	27
3	27	27	27	28	28	28
4	32	16	32	14	7	14
5	11	0	0	21	0	0
6	10	0	5	8	0	4

^a Percentage of materials recovered (accuracy ± 1). Total recovery was $100 \pm 1\%$ in each instance. ^b Percentage yield of nitrophenol (NP). ^c Band 1 contains nitrophenol and nitrophenyl phosphate; the total percentage yield of nitrophenol is equal to the sum of the yields of the two products. The percentage yield of phosphate (P) in this band is equal to the yield of nitrophenyl phosphate alone.

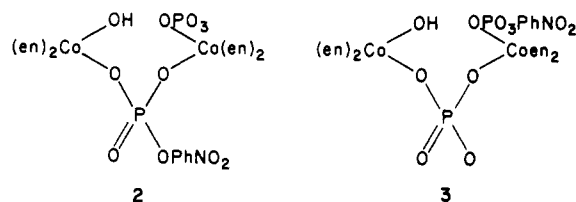
Table VI. Selected $\text{p}K_a$ Values

complex	$\text{p}K_{\text{H}_2\text{O}}^a$	$\text{p}K_p^b$	
$[\text{Co}(\text{en})_2(\text{OH}_2)\text{PO}_4\text{H}]^+$	6.8 ^c	3.1 ^c	9.4 ^c
$[\text{Co}(\text{en})_2(\text{OH}_2)\text{O}_3\text{POC}_6\text{H}_4\text{NO}_2]^+$	7.6 ^d	2.3 ^e	
		6.1 ^f	

^a $\text{p}K_{\text{H}_2\text{O}}$ is the $\text{p}K_a$ of the coordinated water molecule. ^b $\text{p}K_p$ designates the $\text{p}K_a$ values for the oxygen atoms on the phosphate ligand. ^c From data in ref 16. ^d Measured in this work. ^e Estimated for conjugate acid. ^f From data in ref 18.

washings (band 1). Elution of the sorbed products with increasing concentrations of NaClO_4 (up to 0.4 M) resulted in five bands (bands 2–6) that were collected and analyzed for cobalt, nitrophenol, and phosphate. The results are summarized in Table V.

Band 1 contained nitrophenol and nitrophenyl phosphate only. The percentage yields of nitrophenol for the 0.5 and 1.0 M hydrolysis (20% and 12%, respectively) are equal within experimental error to the corresponding values (16% and 12%) calculated from the spectrophotometric kinetic data. Band 2 was identified as *trans*- $[\text{Co}(\text{en})_2(\text{OH}_2)\text{O}_3\text{POC}_6\text{H}_4\text{NO}_2]^+$ by spectrophotometry, ^{31}P NMR, and analytical data (which showed that it contained a 1:1:1 ratio of cobalt, nitrophenol, and phosphate). Band 3 proved to be *cis*- $[\text{Co}(\text{en})_2(\text{OH}_2)\text{O}_3\text{POC}_6\text{H}_4\text{NO}_2]^+$ and confirmed the conclusion from the kinetic studies that this species was a major hydrolysis product of the dimeric starting material. The complex corresponding to band 4 contained cobalt, nitrophenol, and phosphate in a 2:1:2 ratio. Structures 2 and 3 both accommodate the analytical data. They are shown as the hydroxo forms since



deprotonation of $\text{H}_2\text{O-Co}$ would occur in the strongly alkaline media employed for the hydrolysis of the dimeric starting material. The complex which constituted band 4 eluted as a 2+ cation at pH 4. Consideration of the $\text{p}K_a$ values listed in Table VI leads to the expectation that both 2 and 3 would be 2+ cations under the above conditions. Hence it is unlikely that they could be distinguished on the basis of their chromatographic elution behavior.

The hydrolysis ($[\text{OH}^-] = 0.4\text{ M}$) of an aqueous solution of the complex (obtained by concentration of band 4) was studied by ^{31}P NMR (Figure 3). The starting material exhibited peaks at 22.1, 21.8, and 6.2 ppm. The chemical shift of the last peak is

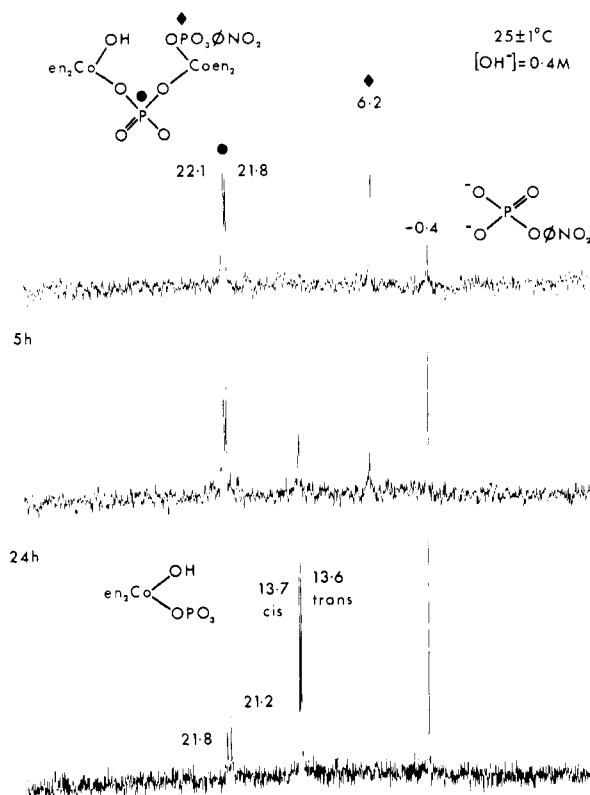
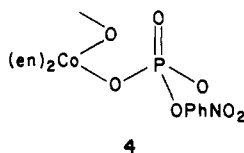
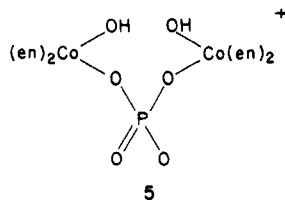


Figure 3. ^{31}P NMR spectra of the base hydrolysis ($[\text{OH}^-] = 0.4 \text{ M}$) of the complex corresponding to band 4 in the product distribution. Spectral parameters: frequency, 24.28 MHz; width, 2083 Hz; pulse angle, 60° ; pulse rate, 1 s.

very similar to those observed for the phosphorus nuclei in the *cis* and *trans* isomers of $[\text{Co}(\text{en})_2(\text{OH})\text{O}_3\text{POC}_6\text{H}_4\text{NO}_2]$ (6.55 and 6.2 ppm, respectively).⁵ This implies that the complex contains a structural unit of type 4. The major nitrophenol-containing



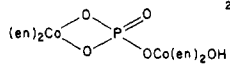
product of the base hydrolysis of band 4 was nitrophenyl phosphate that represented 95% of the nitrophenol present. The remaining 5% was released as free nitrophenol. These results strongly imply that 3 is the correct structure since 2 would be expected to undergo intramolecular hydrolysis in an analogous manner to *cis*- $[\text{Co}(\text{en})_2(\text{OH})\text{O}_3\text{POC}_6\text{H}_4\text{NO}_2]$ to produce nitrophenol as a major product.⁵ The cobalt-containing species produced by nitrophenyl phosphate cleavage from 3 would be 5. The retention of the peaks



near 22 ppm in the ^{31}P NMR spectrum, following the release of nitrophenyl phosphate from 3, is in accord with this expectation. Base hydrolysis of 5 would be expected to yield *cis*- and *trans*- $[\text{Co}(\text{en})_2(\text{OH})\text{PO}_4]$ (both the product distribution and ^{31}P NMR studies confirm this to be the case) and $[\text{Co}(\text{en})_2(\text{OH})_2]^+$. Structure 3 is thus established for the complex corresponding to band 4.

The observation of two signals near 22 ppm and the evidence for the assignment of these signals to a bridging phosphate moiety both need elaboration. The ^{31}P NMR chemical shift for a bridging

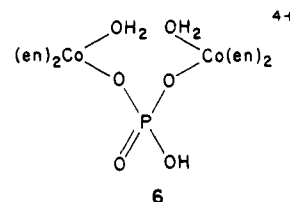
Table VII. Influence of Substituents on ^{31}P NMR Chemical Shifts

compound	δ^a
Na_3PO_4	5.2
$[\text{Co}(\text{NH}_3)_5\text{PO}_4]$	13.8
$[\text{Co}(\text{NH}_3)_5\text{O}_3\text{POC}_6\text{H}_4\text{NO}_2]^+$	6.7
<i>cis</i> - $[\text{Co}(\text{en})_2(\text{OH})\text{PO}_4]^-$	13.7
<i>cis</i> - $[\text{Co}(\text{en})_2(\text{OH})\text{O}_3\text{POC}_6\text{H}_4\text{NO}_2]$	6.6
<i>meso</i> - $[\text{Co}(\text{en})_2(\mu\text{-O}_3\text{POC}_6\text{H}_4\text{NO}_2)_2]^{2+}$	13.7
$\text{Co}(\text{en})_2\text{PO}_4$	23.6 (pH 10)
	33

^a Compound dissolved in 0.2 M NaOH. Chemical shifts measured relative to external 85% H_3PO_4 ($T = 23^\circ\text{C}$).

phosphate ligand can be predicted from an analysis of substituent effects on the chemical shifts of the phosphorus nuclei in the complexes listed in Table VII. The coordination chemical shift ($\Delta\delta$) that is induced on coordination of phosphate with $[\text{Co}(\text{NH}_3)_5]^{3+}$ or $[\text{Co}(\text{en})_2\text{OH}]^{2+}$ is +8.5 ppm; the cobalt-containing moieties can be considered as substituents at the phosphate oxygens. Esterification of one of the complexes phosphate oxygens with 4-nitrophenol is responsible for a -7 ppm contribution to the chemical shift. This is true for both the pentaammine⁶ and bis(1,2-ethanediamine)phosphate ester complexes.⁵ The chemical shift of the phosphorus nucleus in 5 can be regarded as arising from coordination of the $[\text{Co}(\text{en})_2(\text{OH})]^{2+}$ moiety with one of the oxygen atoms of the parent $[\text{Co}(\text{en})_2(\text{OH})\text{PO}_4]^-$ complex. It is therefore predicted that the chemical shift will be equal to ~ 22 ppm ($13.7 + 8.5$). Alternatively, the complexation of two of the $[\text{Co}(\text{en})_2(\text{OH})]^{2+}$ moieties with two of the oxygen atoms of PO_4^{2-} yields a similar predicted shift of 22 ppm. The good agreement between the calculated and observed values suggests that the additivity of ^{31}P NMR chemical shifts has considerable predictive utility for systems of the present type. The probable reason for the observation of two peaks near 22 ppm is the occurrence of *cis* and *trans* geometries about the cobalt centers. The origin of these isomers is discussed later.

Band 5 in the product distribution experiments was identified as $[\text{Co}(\text{en})_2(\text{OH})_2]^{3+}$ by spectrophotometry. Elemental analysis confirmed that it contained no phosphate or nitrophenol. Band 6 contained cobalt and phosphate in a 2:1 ratio and behaved as a 4+ cation on the ion-exchange column. The absorption spectrum of an aqueous solution of the complex at pH 4 ($\lambda_{\text{max}} = 506$, $\lambda_{\text{min}} = 428$, $\mu_{\text{max}} = 361$ nm) is very similar to that of an authentic sample of *cis*- $[\text{Co}(\text{en})_2(\text{OH})_2\text{PO}_4\text{H}]^+$ under the same conditions ($\lambda_{\text{max}} = 509$, $\lambda_{\text{min}} = 428$, $\lambda_{\text{max}} = 364$ nm). The most likely structure for this species is 6; that is, the protonated form of 5 (the extent of protonation was predicted from the pK_a values listed in Table VI).



Product Distribution and Kinetic Studies by ^{31}P NMR Spectroscopy. Initial experiments were performed on a diastereoisomeric mixture of the bis(μ -nitrophenyl phosphato) dimers. The spectra obtained for the hydrolysis in 0.2 M OH^- are illustrated in Figure 4 and the chemical shifts and assignments for the peaks are listed in Table VIII. The initial spectrum was accumulated over a period of ca. $4t_{1/2}$ for the rapid nitrophenol-producing step. The observed species are thus the major products of this reaction (a small amount of starting material A is also present). Peaks C and C' have chemical shifts that are characteristic of 3. In this series of spectra the nitrophenyl phosphate resonance of 3 (C') is coincident with that for *trans*- $[\text{Co}(\text{en})_2(\text{OH})\text{O}_3\text{POC}_6\text{H}_4\text{NO}_2]$ (E) but in other spectra, which were obtained at higher resolution

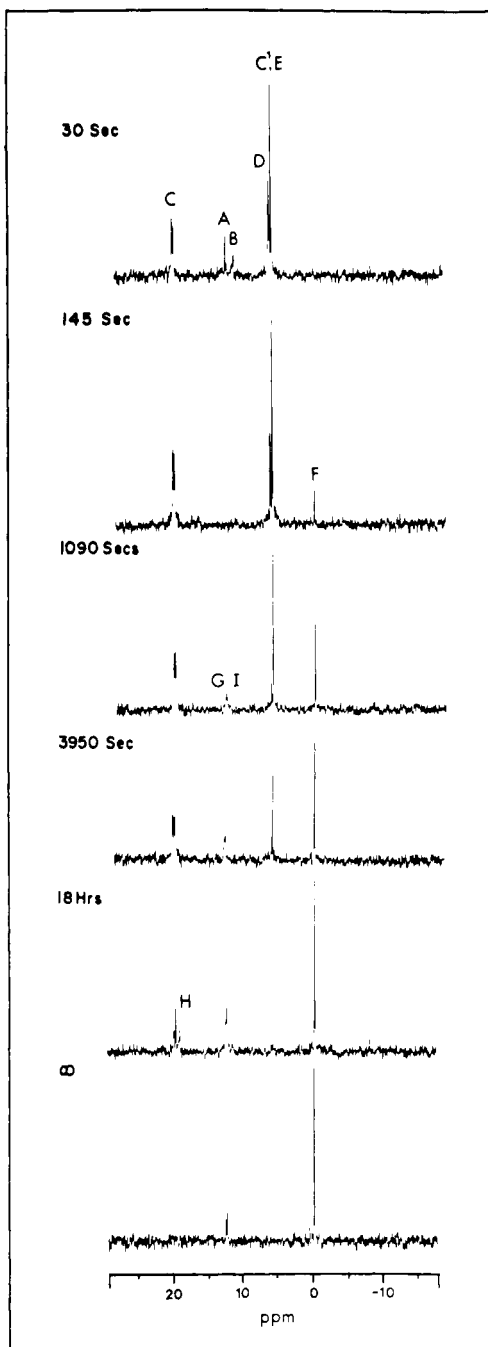


Figure 4. ^{31}P NMR spectra for the base hydrolysis ($[\text{OH}^-] = 0.2 \text{ M}$) of $\{[\text{Co}(\text{en})_2(\mu\text{-O}_3\text{POC}_6\text{H}_4\text{NO}_2)]_2\}^{2+}$ (diastereoisomeric mixture) ($T = 27 \pm 1 \text{ }^\circ\text{C}$). Accumulation of each spectrum was started at the time indicated. Spectral parameters: frequency, 40.3 MHz; bandwidth, 2100 Hz; pulse angle, 60° ; pulse rate, 1 s; 4K data points; 100 transients per spectrum.

(see later), these two peaks were separated. Peak D has a chemical shift that is characteristic of $\text{cis-}[\text{Co}(\text{en})_2(\text{OH})\text{O}_3\text{POC}_6\text{H}_4\text{NO}_2]$. Peak B is associated with the short induction period and disappears in the second spectrum. The nature of the species that gives rise to this resonance is discussed later. Very little nitrophenyl phosphate (F) is released early in the reaction sequence. $\text{cis-}[\text{Co}(\text{en})_2(\text{OH})\text{O}_3\text{POC}_6\text{H}_4\text{NO}_2]$ undergoes hydrolysis to release nitrophenyl phosphate (F) (plus $[\text{Co}(\text{en})_2(\text{OH})_2]^+$) and $\text{cis-}[\text{Co}(\text{en})_2(\text{OH})\text{PO}_4]^-$ (G) (plus nitrophenol). The corresponding trans isomer also undergoes hydrolysis, but at a much slower rate, to liberate mainly nitrophenylphosphate via Co–O cleavage. By 3950 s **3** is the sole remaining cobalt complex that contains nitrophenyl phosphate. cis- and $\text{trans-}[\text{Co}(\text{en})_2(\text{OH})\text{PO}_4]^-$ (G, H) and nitrophenyl phosphate (F) are the final products after 24 h ($t = \infty$). The hydrolysis products for the 1.0 M hydroxide reaction

Table VIII. ^{31}P NMR Spectral Assignments for the Spectra Shown in Figures 4, 5, and 6

peak	chem shift, ^a ppm	assignment
A	13.40	$\text{meso-} \{[\text{Co}(\text{en})_2(\mu\text{-O}_3\text{POC}_6\text{H}_4\text{NO}_2)]_2\}^{2+}$
B	12.25, 13.35	$\text{rac-} \{[\text{Co}(\text{en})_2(\mu\text{-O}_3\text{POC}_6\text{H}_4\text{NO}_2)]_2\}^{2+}$
C	12.20	?
C'	21.75, 21.98	$\text{O}_3\text{P}^*\text{OPhNO}_2$
C ^{1*}	6.22	
D	6.60	$\text{cis-}[\text{Co}(\text{en})_2(\text{OH})\text{O}_3\text{POC}_6\text{H}_4\text{NO}_2]$
E	6.22	$\text{trans-}[\text{Co}(\text{en})_2(\text{OH})\text{O}_3\text{POC}_6\text{H}_4\text{NO}_2]$
F	-0.38	4-nitrophenyl phosphate
G	13.76	$\text{cis-}[\text{Co}(\text{en})_2(\text{OH})\text{PO}_4]^-$
H	20.97	
I	13.63	$\text{trans-}[\text{Co}(\text{en})_2(\text{OH})\text{PO}_4]^-$

^a Chemical shift precision is ± 0.05 ppm.

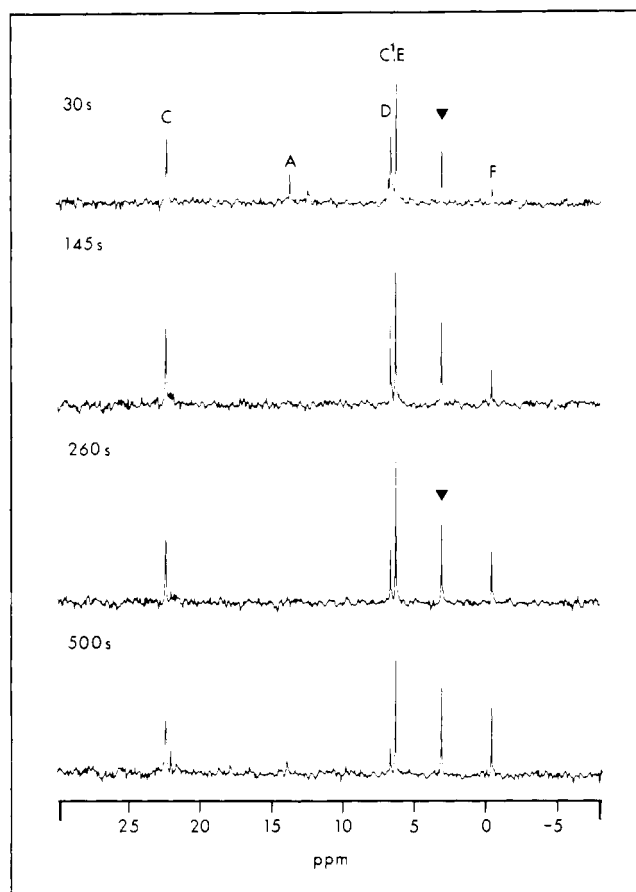


Figure 5. ^{31}P NMR spectra for the base hydrolysis ($[\text{OH}^-] = 0.2 \text{ M}$) of $\text{meso-} \{[\text{Co}(\text{en})_2(\mu\text{-O}_3\text{POC}_6\text{H}_4\text{NO}_2)]_2\}^{2+}$ ($T = 25 \pm 1 \text{ }^\circ\text{C}$). Spectral parameters are identical with those in Figure 4, and the peak assignments are listed in Table VIII. Trimethyl phosphate (\blacktriangledown) was used as the internal reference.

are the same as for the 0.2 M hydrolysis, the only difference being their relative yields.

The hydrolysis of the individual diastereoisomers in 0.2 M hydroxide was also studied, and the spectra for the *meso* and *rac* forms appear in Figures 5 and 6, respectively. Both diastereoisomers clearly yield the same products. The peak-labeling scheme

Table IX. ^{31}P NMR Spectral Assignments for Figures 7 and 8 ($T = 5 \pm 1^\circ\text{C}$)

peak	diastereoisomer		assignment
	δ (meso) ^a	δ (racemic) ^a	
A	13.31	13.16, 13.26	reactant
B	12.11	11.76, 12.11, 12.44, 12.62	?
B ¹	6.48, 6.53	6.45, 6.53, 6.58	?
C	31.15	31.38	?
C ¹	6.30	6.30	?
D	6.35	6.35	<i>cis</i> -[Co(en) ₂ (OH)O ₃ POC ₆ H ₄ NO ₂]
E	21.69 ¹	21.46, 21.71	
E ₁	5.95 [*]	5.95	<i>trans</i> -[Co(en) ₂ (OH)O ₃ POC ₆ H ₄ NO ₂] nitrophenyl phosphate
F	6.00	6.00	
G	-0.73	-0.78	

^a Chemical shift precision is ± 0.05 ppm.

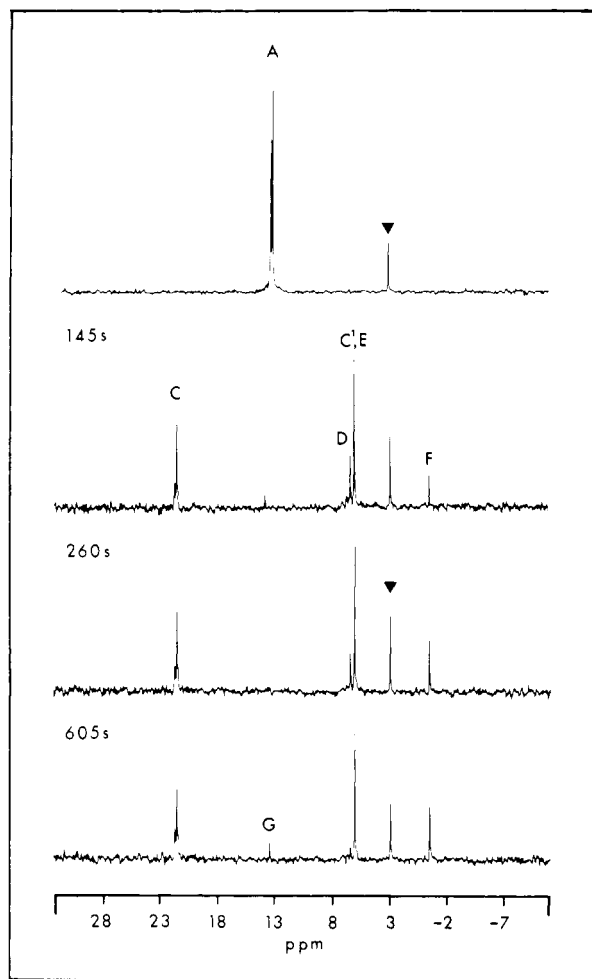


Figure 6. ^{31}P NMR spectra for the base hydrolysis ($[\text{OH}^-] = 0.2 \text{ M}$) of *rac*- $\{[\text{Co}(\text{en})_2(\mu\text{-O}_3\text{POC}_6\text{H}_4\text{NO}_2)]_2\}^{2+}$ ($T = 25 \pm 1^\circ\text{C}$). Spectral parameters are identical with those in Figure 4, and the peak assignments are listed in Table VIII. Internal reference was trimethyl phosphate (▼).

is the same as that used in Figure 4, and hence Table VIII provides the required chemical shift and peak identification data.

In order to study the initial fast reaction, a series of low-temperature ^{31}P NMR spectra for each of the diastereoisomers was obtained; the 0.2 M hydroxide experiments were repeated at 5°C . The spectra for the meso and rac forms are illustrated in Figures 7 and 8. The chemical shifts and assignments for each series of spectra are listed in Table IX. The data for the meso form will be discussed first since the spectra are somewhat simpler than those of the rac diastereoisomer. An enlargement of the spectrum obtained at 750 s in this series is reproduced in Figure

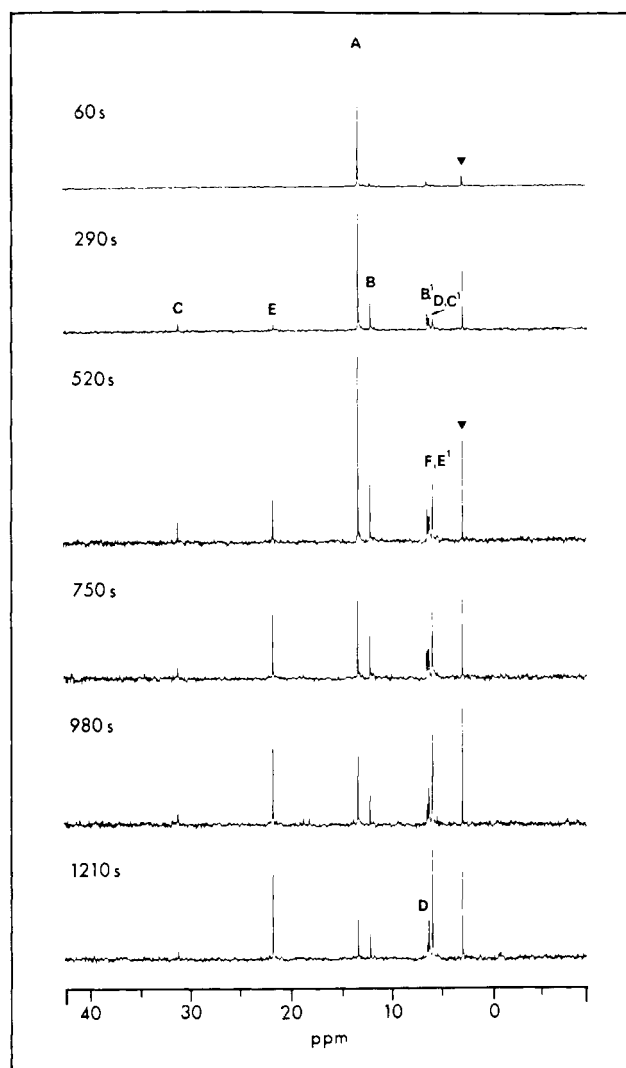


Figure 7. ^{31}P NMR spectra for the base hydrolysis ($[\text{OH}^-] = 0.2 \text{ M}$) of *meso*- $\{[\text{Co}(\text{en})_2(\mu\text{-O}_3\text{POC}_6\text{H}_4\text{NO}_2)]_2\}^{2+}$ at $5 \pm 1^\circ\text{C}$. Internal reference was trimethyl phosphate (▼). Peak assignments are listed in Table X.

9. Peaks A, D, E, E¹, and F have already been assigned. The species that give rise to the signals B, B¹, C, and C¹ remain to be established, and it is of particular interest whether or not these species are directly associated with nitrophenol production. A partial answer to this question was obtained from a study of the base hydrolysis of *meso*- $\{[\text{Co}(\text{en})_2(\mu\text{-O}_3\text{POC}_6\text{H}_5)]_2\}^{2+}$ for which no ester hydrolysis occurs and the sole final phosphate-containing product is phenyl phosphate (Figure 10). The major initial

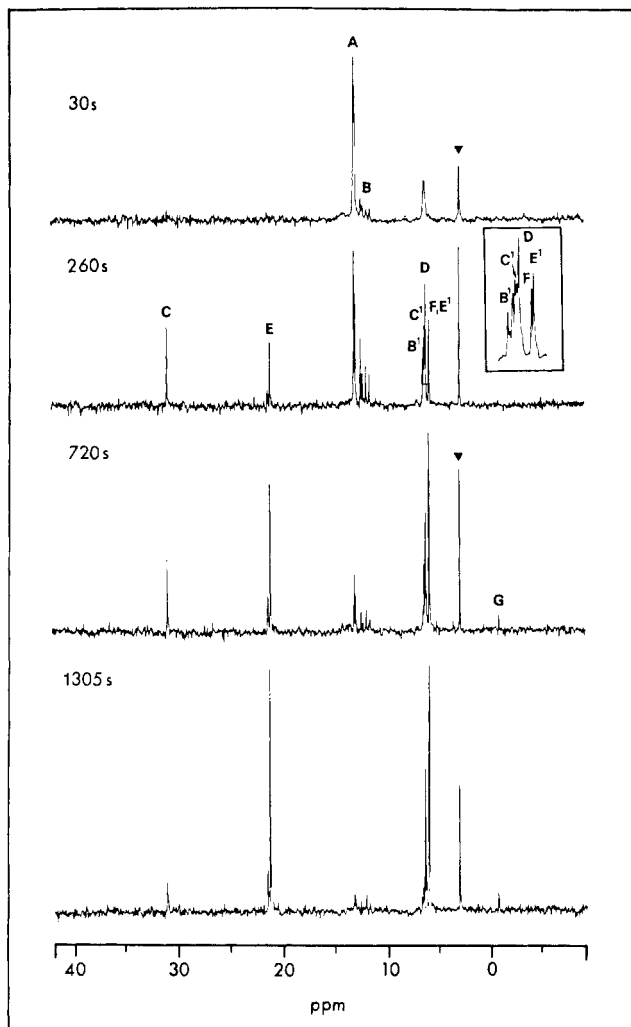


Figure 8. ^{31}P NMR spectra for the base hydrolysis ($[\text{OH}^-] = 0.2 \text{ M}$) of $\text{rac}-[[\text{Co}(\text{en})_2(\mu\text{-O}_3\text{POC}_6\text{H}_4\text{NO}_2)]_2]^{2+}$ at $5 \pm 1^\circ\text{C}$. Internal reference was trimethyl phosphate (\blacktriangledown). Peak assignments are listed in Table IX. The inset contains an expansion of the spectrum around 6 ppm.

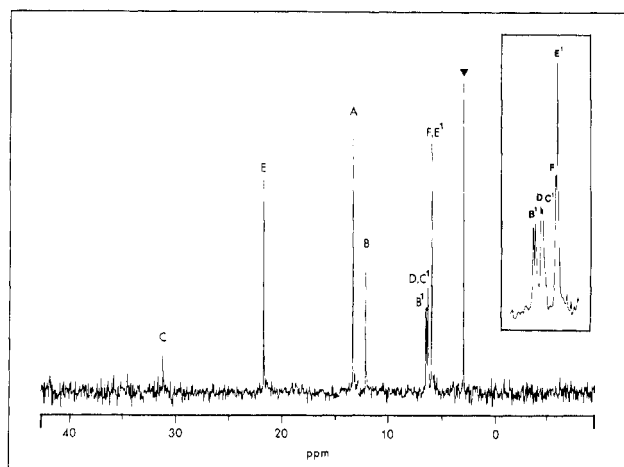


Figure 9. Enlargement of the 750 s spectrum in Figure 7. Inset contains an expansion of the spectrum around 6 ppm. Internal reference was trimethyl phosphate (\blacktriangledown).

reaction products are *cis*- and *trans*- $[\text{Co}(\text{en})_2(\text{OH})\text{O}_3\text{POC}_6\text{H}_5]$ at 7.4 and 7.0 ppm, respectively (starting material, 14.7 ppm). The peaks at 13.6 and 7.6 ppm appear to be analogous to B and B' that are observed initially in the hydrolysis of the nitrophenyl phosphate dimers. The *cis*- and *trans*-hydroxophosphate ester products are apparently produced from the species corresponding to

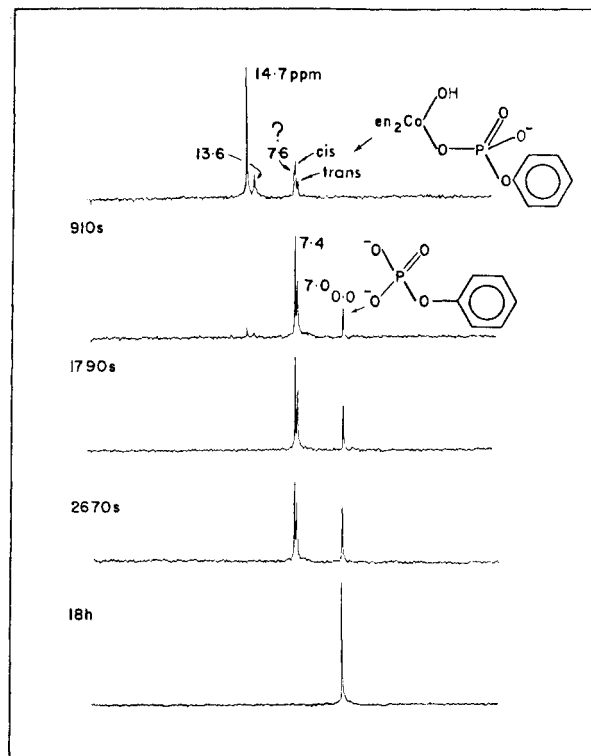


Figure 10. ^{31}P NMR spectra for the base hydrolysis ($[\text{OH}^-] = 0.2 \text{ M}$) of $\text{meso}-[[\text{Co}(\text{en})_2(\mu\text{-O}_3\text{POC}_6\text{H}_5)]_2]^{2+}$ ($T = 15 \pm 1^\circ\text{C}$).

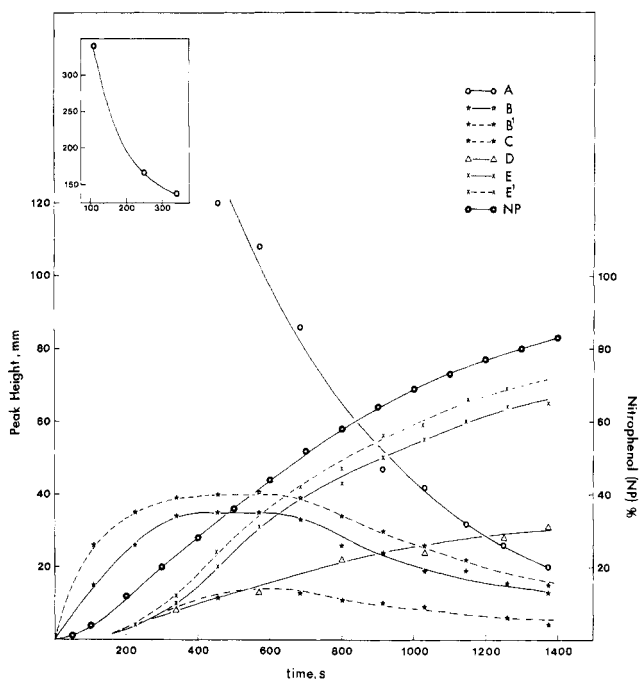


Figure 11. Product-time profiles for the base hydrolysis of $\text{meso}-[[\text{Co}(\text{en})_2(\mu\text{-O}_3\text{POC}_6\text{H}_4\text{NO}_2)]_2]^{2+}$ in 0.2 M OH^- at $5 \pm 1^\circ\text{C}$. The left-hand ordinate refers to the normalized peak heights obtained from the ^{31}P NMR kinetic studies (see text), and the right-hand ordinate refers to the yield of nitrophenol measured spectrophotometrically as a function of time.

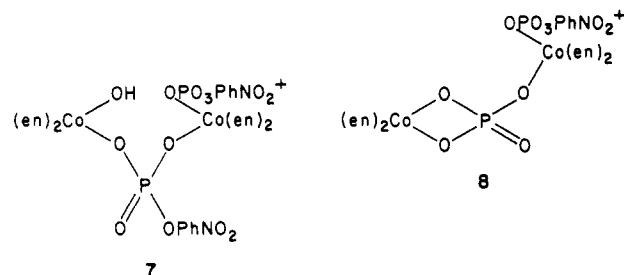
to these peaks in a rapid second step. Therefore, these peaks appear to represent intermediates that are involved in the cleavage of the dimer into its monomeric units and are not uniquely associated with ester hydrolysis. In contrast, the peak near 31 ppm is absent in the phenyl phosphate spectra and hence must be directly involved in ester hydrolysis. The peaks that would correspond to the analogue of **3** are also absent. This must be the case since the species would be formed by hydrolysis of the

bridging phosphate ester and no ester hydrolysis is observed for the phenyl phosphate dimer.

Thirteen spectra were obtained for the hydrolysis of the *meso*-bis(μ -nitrophenyl phosphato) dimer at 5 °C in 0.2 M hydroxide solution (a representative five are reproduced in Figure 7). The product-time profiles are plotted in Figure 11. The production of nitrophenol was monitored spectrophotometrically at 5 °C, and the percentage yield of this species (normalized to 100% for the rapid step of the reaction under investigation) as a function of time is superimposed on the ^{31}P NMR profiles. This allows a direct comparison to be made between the kinetics of nitrophenol release and the appearance of the phosphorus-containing products of the reaction.

During the induction period (prior to the release of nitrophenol) the starting material A is converted into the species corresponding to peaks B and B¹. The concentration of this species rapidly attains a steady state. The growth of C initially parallels nitrophenol release, but then it also reaches an apparent steady-state concentration. Peaks E and E¹ (which are due to 3) and peak D (*cis*-[Co(en)₂(OH)O₃POC₆H₄NO₂]) parallel nitrophenol production throughout the course of the reaction. Approximate values for the rates of disappearance of starting material and appearance of E and E¹ can be calculated from the data; a computer fit of the data indicates a first-order rate law. The rate constants are as follows: disappearance of starting material, $5.6 (\pm 0.9) \times 10^{-3} \text{ s}^{-1}$; appearance of peak E, $1.2 (\pm 0.3) \times 10^{-3} \text{ s}^{-1}$; appearance of peak E¹, $1.4 (\pm 0.3) \times 10^{-3} \text{ s}^{-1}$. The large errors associated with the rate constants result from the considerable uncertainty attached to the measurements of peak heights ($\pm 10\%$) in the NMR spectra. The spectrophotometrically determined rate constant for nitrophenol production at 5 °C is $1.19 (\pm 0.05) \times 10^{-3} \text{ s}^{-1}$. The agreement between the rate of appearance of E and E¹ and nitrophenol production provides further evidence that 3 is directly a result of the pathway that leads to the release of nitrophenol. Peaks B, B¹, and C maintain near steady-state levels for 400–600 s and then begin to decay. This coincides with exhaustion of the starting material.

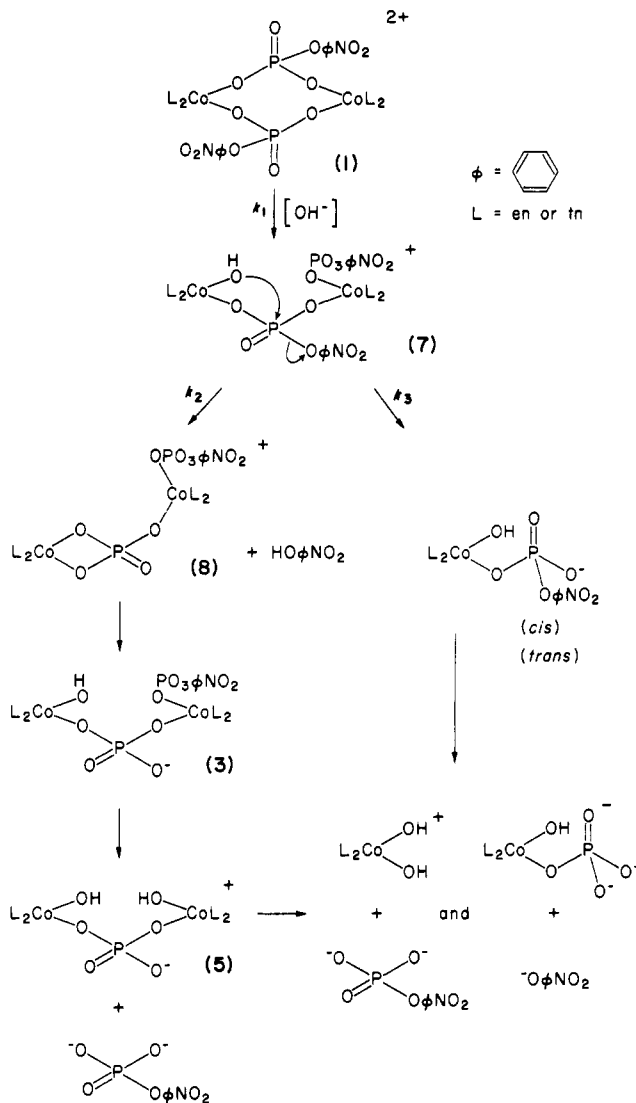
An assignment for the species generated early in the reaction sequence can be proposed on the basis of the data presented above. Complex 7 is produced from starting material without nitrophenol



release by base-catalyzed Co–O cleavage. This can then decompose to *cis*- and *trans*-[Co(en)₂(OH)O₃POC₆H₄NO₂] or undergo intramolecular hydrolysis to release nitrophenol and generate 8. The phosphate chelate ring in 8 would then be expected to open rapidly (by analogy with [Co(en)₂PO₄]^{5,16}) under the strongly basic conditions to yield 3.

The ^{31}P NMR chemical shift expected for the bridging phosphate group in 8 can be estimated by means of the "additivity" procedure outlined previously. Structure 8 can be regarded as being derived from 3 by the formation of a phosphate chelate ring. The Co(en)₂(O)O₃POC₆H₄NO₂ moiety is common to both complexes. Formation of [Co(en)₂PO₄] from the monodentate phosphate complex [Co(en)₂(OH)PO₄] results in a 10 ppm downfield shift of the phosphorus resonance (Table VII). The predicted chemical shift for the bridging phosphate in 8 is thus 31.8 ppm (21.8 + 10). The peak at 31.2 ppm (C) in Figures 7 and 8 is thus assigned to the chelating and bridging phosphate ligand of 8. The resonance of the nonbridging nitrophenyl phosphate moiety in 8 would be expected to lie in the range 6.2–6.8 ppm, that is, have a chemical shift that is characteristic for monodentate nitrophenyl phosphate. Similarly, the chemical shift

Scheme I



of the bridging phosphate ester in 7 is predicted to be close to that of the starting material and the resonance of the nonbridging ester to lie between 6.2 and 6.8 ppm. On the basis of the above chemical shift analyses and the product-time profiles in Figure 11, the remaining peaks in the ^{31}P NMR spectra can be assigned: B and B¹ to 7, and C and C¹ to 8.

Discussion

Scheme I (L = en) summarizes the essential features of the reaction mechanism elucidated from the kinetic, product distribution, and ^{31}P NMR studies discussed above. In a rapid first step, the eight-membered ring of the dimer 1 is opened by conjugate base cleavage of one of the Co–O bonds to yield 7 (k_1). This species is then consumed in the second step by intramolecular attack of coordinated hydroxide at the bridging phosphate ester to yield 8 and nitrophenol (k_2) or by Co–O bond rupture to yield *cis*- and *trans*-[Co(en)₂(OH)O₃POC₆H₄NO₂] (k_3). The latter complex hydrolyzes slowly to liberate nitrophenol (plus *cis*- and *trans*-[Co(en)₂(OH)PO₄][−]) and nitrophenyl phosphate (plus [Co(en)₂(OH)₂]⁺) whereas 8 is rapidly converted to 3 by case-catalyzed chelate-ring opening. Base-catalyzed Co–O cleavage of the cobalt–phosphate ester bond in 3 yields 5 that slowly decomposes to *cis*- and *trans*-[Co(en)₂(OH)PO₄][−] plus *cis*- and *trans*-[Co(en)₂(OH)₂]⁺. The nitrophenyl phosphate, which was isolated after the base hydrolysis reaction ([OH[−]] = 0.4 M), had been allowed to proceed for 2 h in H₂¹⁸O, contained no ¹⁸O label. This result indicates that very largely Co–O bond rupture occurs during its formation and thus supports the above mechanism. A sample of nitrophenol was also isolated from this reaction and was

Scheme II

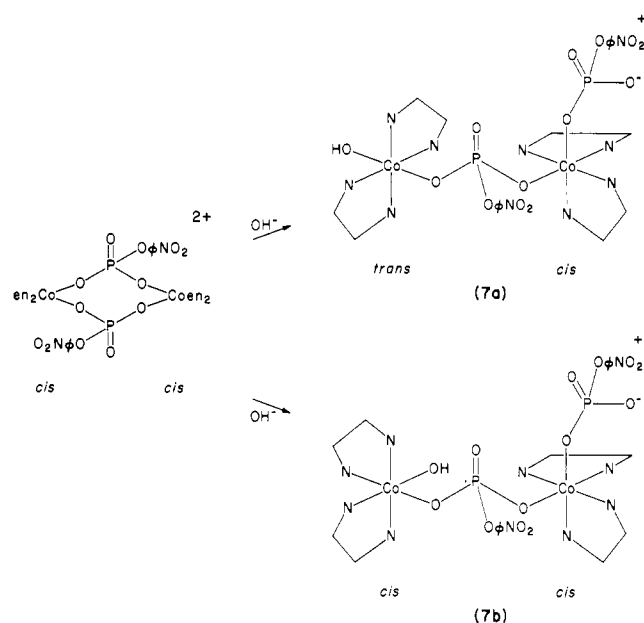


Table X. Product Distribution Data for the Base Hydrolysis ($[\text{OH}^-] = 0.5 \text{ M}$) of $\text{rac-}[\text{Co}(\text{en})_2(\mu\text{-O}_3\text{POC}_6\text{H}_4\text{NO}_2)]_2^{2+}$ ($T = 25^\circ \text{C}$)

band	compound	yield, ^a %		
		Co ^b	NP ^c	P ^d
1	(a) 4-nitrophenol	0	20	
	(b) 4-nitrophenyl phosphate	0	17	17
2	<i>trans</i> -[Co(en) ₂ (OH)O ₃ POC ₆ H ₄ NO ₂]	23	23	23
3	<i>cis</i> -[Co(en) ₂ (OH)O ₃ POC ₆ H ₄ NO ₂]	27	27	27
4	3	32	16	32
5	[Co(en) ₂ (OH) ₂] ⁺	11	0	0
6	4	10	0	5

^a Accuracy ± 1 . ^b Cobalt. ^c 4-Nitrophenol. ^d Phosphate.

found to contain no ¹⁸O, thus confirming that ester hydrolysis proceeds via a mechanism which results in P–O cleavage and not C–O rupture.

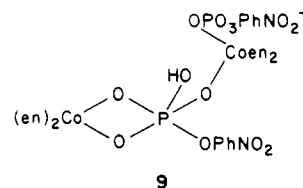
One feature that requires further elaboration is the splitting observed in the ³¹P NMR peaks assigned to **7**. Both cobalt starting materials have a *cis* arrangement of the two phosphate esters. A conventional S_N1cB process¹⁹ is responsible for Co–O cleavage in the first step of the reaction, and consequently *cis* to *trans* isomerization can take place at the cobalt center that is involved. Two products **7a** and **7b** can thus arise from the ring-opening reaction (Scheme I), and they would be expected to differ in their ³¹P NMR chemical shifts. The *trans,cis* isomer **7a** is a “dead-end” species since it is geometrically impossible for the coordinated hydroxide to participate in intramolecular hydrolysis of the bridging phosphate ester. Rapid Co–O cleavage then leads to the production of *cis*- and *trans*-[Co(en)₂(OH)O₃POC₆H₄NO₂]. However, in the *cis,cis* isomer **7b**, intramolecular hydrolysis of the bridging phosphate ester will compete with production of *cis*- and *trans*-[Co(en)₂(OH)O₃POC₆H₄NO₂] by the S_N1cB path. The two peaks near 22 ppm, which are ultimately observed for the bridging phosphate ligand in **3**, are presumably also due to the existence of *cis,cis* and *cis,trans* configurations around two cobalt centers.

The quantitative product distribution data for the hydrolysis of $\text{rac-}[\text{Co}(\text{en})_2\text{O}_3\text{POC}_6\text{H}_4\text{NO}_2]_2^{2+}$ in 0.5 M hydroxide is tabulated in Table X together with the structures of the complexes corresponding to each of the bands produced by the cation-exchange chromatography procedure. If Scheme I is correct, then there are two conditions that the product distribution must satisfy: (i) The total yield of nitrophenol must be equal to the amount

of nitrophenol released during the formation of **3**. The latter value is given by the sum of half of the percentage yield of cobalt in **3** plus half of the percentage yield of cobalt in **5** (since **5** is produced from **3** during the course of the reaction). The calculated yield of nitrophenol is thus 21 (± 1)%. (ii) The yield of nitrophenyl phosphate must equal the sum of the yield of [Co(en)₂(OH)₂]⁺ and half of the yield of cobalt in **5** (since **5** is generated from **3** by the release of 1 mol of nitrophenyl phosphate). The observed yield is 17 (± 1)% and the calculated yield is 16 (± 2)%.

Convincing evidence for the participation of a complex of type **7b** in the base hydrolysis of the dimer is provided by the results of a spectrophotometric kinetics experiment. The *meso* diastereoisomer was hydrolysed for 20 s (ca. $1/2 t_{1/2}$ for nitrophenol production) in 0.2 M hydroxide solution and then quenched to pH 4. If **7b** is the negative species, then it would be expected to exhibit a similar pH–rate profile to that observed for the hydrolysis of *cis*-[Co(en)₂(OH)₂O₃POC₆H₄NO₂], that is, have a pH-independent rate maximum.⁶ The quenching procedure described above should trap **7b** in its unreactive protonated form if it is present in solution. If the pH is raised above the pK_a of the coordinated water, the reactive form of the complex would be generated and rapid intramolecular hydrolysis of the bridging ester would ensue. Moreover, an induction period should not be observed since **7b** is already present. When the pH 4 solution from above was mixed with buffers to yield final pH values of 9.1, 9.8, 10.3, and 10.8 (with tris/HClO₄, diethanolamine/HClO₄, ammonia/HClO₄, and triethylamine/HClO₄, respectively), rapid release of nitrophenol was observed. There was no induction period, and the rate was independent of pH ($k_2 = 2.1 (\pm 0.2) \times 10^{-2} \text{ s}^{-1}$, 25 °C). A control experiment under the same conditions at pH 10 with the dimer as the substrate yielded a rate constant of only $2.15 (\pm 0.03) \times 10^{-5} \text{ s}^{-1}$. More importantly, there was no induction period. The reactive intermediate **7b** must initially be produced by Co–O cleavage before ester hydrolysis can occur. The rate of this reaction (k_1) is dependent on the concentration of hydroxide ion since it proceeds via an S_N1cB mechanism. However, once **7b** is present, it will react rapidly (with rate constant k_2) in the hydroxo form. It has been shown above that the pK_a of the coordinated water must be less than 9; it is probably somewhat less than the value of 7.6 that was observed for *cis*-[Co(en)₂(OH)₂O₃POC₆H₄NO₂]⁺.⁵ Therefore, k_2 should be constant above pH 8.5 whereas k_1 should be linearly dependent on hydroxide concentration over the whole pH range studied. Since an induction period is observed for nitrophenol release in strong base, it follows that k_1 must be larger than k_2 under those conditions. The absence of an induction period for the reaction at pH 10 implies that, under these conditions, $k_1 < k_2$ and that production of **7** has become rate determining.

The intramolecular hydrolysis of the bridging phosphate ester in **7b** presumably takes place via the formation of a pentaoxyphosphorane intermediate (or transition state) of type **9**. The

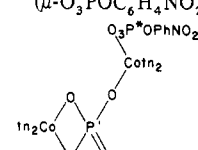
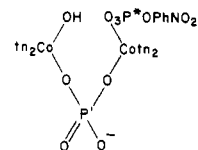


detailed chemistry associated with this type of mechanism has been discussed previously with respect to the analogous intramolecular hydrolyses^{5,6} of [Co(NH₃)₃O₃POC₆H₄NO₂]⁺ and *cis*-[Co(en)₂(OH)O₃POC₆H₄NO₂]. The observation that ester hydrolysis proceeds with complete P–O bond rupture is in accord with this mechanism.

The base hydrolysis rates of *meso*- and *rac*-[Co(en)₂(μ-O₃POC₆H₄NO₂)₂]²⁺ exhibit similar deviations from linearity (Figure 2) above 0.5 M hydroxide to that observed for *cis*-[(en)₂(OH)O₃POC₆H₄NO₂].⁵ Possible explanations involving intramolecular attack of deprotonated coordinated hydroxide, intramolecular attack of hydroxide, or generation of hexacoordinate intermediates can be advanced to account for the

(19) Jackson, W. G.; Sargeson, A. M. “Rearrangements in Ground and Excited States”; de Mayo, P., Ed.; Academic Press: New York, 1980; Vol. 2, pp 273–378.

Table XI. Peak Assignments for the ^{31}P NMR Spectra in Figure 12

peak	chem shift, ppm	assignment
A	9.93, 10.13	<i>meso-</i> and <i>racemic-</i> $\{[\text{Co}(\text{tn})_2(\mu\text{-O}_3\text{POC}_6\text{H}_4\text{NO}_2)]_2\}^{2+}$
B	30.95, 31.18'	
B'	5.08*	
C	19.03, 20.11'	
C'	4.90*	
D	5.79	?
E	5.36	<i>cis-</i> $[\text{Co}(\text{tn})_2(\text{OH})\text{O}_3\text{POC}_6\text{H}_4\text{NO}_2]$
F	5.08	<i>trans-</i> $[\text{Co}(\text{tn})_2(\text{OH})\text{O}_3\text{POC}_6\text{H}_4\text{NO}_2]$
G	-0.73	nitrophenyl phosphate
H	12.75	$[\text{Co}(\text{tn})_2(\text{OH})\text{PO}_4]$

observations. However, insufficient data²⁰ are available to make a choice between these alternatives and this aspect will not be pursued further here.

It has been shown in the present work that the complex obtained by coordination of *p*-nitrophenyl phosphate to the bis(1,3-propanediamine)cobalt(III) moiety in a previous study has a structure that is analogous to that found for $\{[\text{Co}(\text{en})_2(\mu\text{-O}_3\text{POC}_6\text{H}_4\text{NO}_2)]_2\}^{2+}$. Thus the previously proposed mechanism for hydrolysis of the 1,3-propanediamine (tn) complex is in error since it was based on the belief that this complex was monomeric. ^{31}P NMR studies of the base hydrolysis of the nitrophenyl phosphate complex (Figure 12) confirmed that the mechanism is similar to that observed for the $\{[\text{Co}(\text{en})_2(\mu\text{-O}_3\text{POC}_6\text{H}_4\text{NO}_2)]_2\}^{2+}$ dimer (Scheme I with L = tn). Assignments for the spectra in Figure 12 are listed in Table XI. The $\{[\text{Co}(\text{tn})_2(\mu\text{-O}_3\text{POC}_6\text{H}_4\text{NO}_2)]_2\}^{2+}$ dimer hydrolyzes ~ 50-fold faster (as measured by nitrophenol release) than its ethanediamine analogue. This result is in keeping with the general observation that substitution in bis(1,3-propanediamine) complexes is more rapid than the corresponding bis(1,2-ethanediamine) complexes,²¹ but it also requires a more rapid intramolecular attack of coordination OH^- on the nitrophenyl phosphate bridging the two Co ions by a factor of about 20.

Concluding Remarks

An important mechanistic aspect of the dimeric systems is that ester hydrolysis occurs exclusively via an intramolecular pathway; the intermolecular attack of hydroxide ion at the phosphorus atoms of the dimer does not compete with this process, even under strongly basic conditions (that is, when $[\text{OH}^-] = 1 \text{ M}$). This result is consistent with the chemistry observed^{5,6} for $[\text{Co}(\text{NH}_3)_5\text{O}_3\text{POC}_6\text{H}_4\text{NO}_2]^+$ and *cis*- $[\text{Co}(\text{en})_2(\text{OH})_2\text{O}_3\text{POC}_6\text{H}_4\text{NO}_2]^+$. The $\{[\text{Co}(\text{en})_2(\mu\text{-O}_3\text{POC}_6\text{H}_4\text{NO}_2)]_2\}^{2+}$ dimer also provides a unique opportunity to assess the effect that simultaneous coordination to two metal centers has on the rate of phosphate ester hydrolysis. The rates of intramolecular hydrolysis for **7b** and *cis*- $[\text{Co}(\text{en})_2(\text{OH})\text{O}_3\text{POC}_6\text{H}_4\text{NO}_2]$ are $2 \times 10^{-2} \text{ s}^{-1}$ and $7.8 \times 10^{-4} \text{ s}^{-1}$, respectively.⁵ Thus, the presence of a second cobalt center in **7b** is responsible for a 26-fold increase in rate over that observed for the mononuclear complex. This result enables an estimate of the relative contributions of "phosphate charge neutralization" and "intramolecular" (pro-

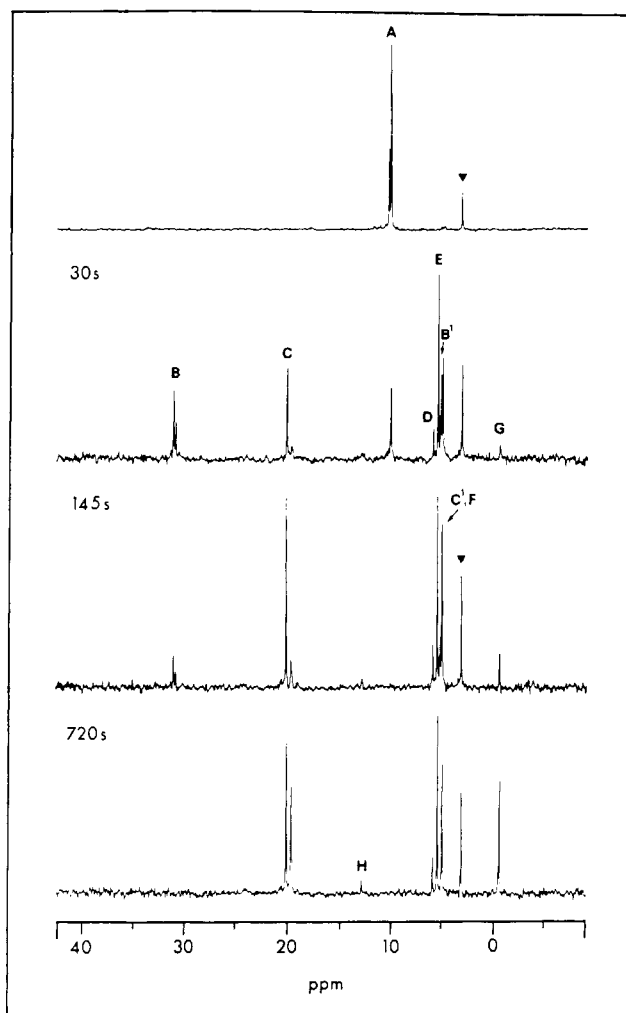


Figure 12. ^{31}P NMR spectra for the base hydrolysis ($[\text{OH}^-] = 0.2 \text{ M}$) of $\{[\text{Co}(\text{tn})_2(\mu\text{-O}_3\text{POC}_6\text{H}_4\text{NO}_2)]_2\}^{2+}$ at $5 \pm 1^\circ \text{C}$. Internal reference was trimethyl phosphate (▼). Peak assignments are listed in Table XI.

pinquity) components to the rate enhancements observed for the hydrolysis of coordinated nitrophenyl phosphate relative to the uncoordinated ester. The rate of hydrolysis of uncomplexed nitrophenyl phosphate is approximately $2 \times 10^{-9} \text{ s}^{-1}$ (25°C) over the pH range 9–13.5.²² Thus, the rate enhancement is 4×10^5 -fold for *cis*- $[\text{Co}(\text{en})_2(\text{OH})\text{O}_3\text{POC}_6\text{H}_4\text{NO}_2]$ of which $\sim 10^4$ is estimated to be due to the intramolecular component and the remainder to the effect of Co(III). In a similar analysis for the (tn)₂ complex the intramolecular effect is approximately 10^6 . The conclusion from these analyses is that monodentate coordination of a phosphate ester to a metal ion will not, by itself, lead to a large acceleration in the rate of ester hydrolysis although rate enhancements as large as 400-fold have been observed for coordinated phosphate triesters.²³ The dominant role of the metal ion in the systems discussed above is to provide a template on which the nucleophile and phosphate ester are held in close proximity, thus enabling facile intramolecular hydrolysis to occur.

The role of metal ions in the hydrolytic enzymic systems might then be seen to be several fold. They can group the reactants and provide a coordinated nucleophile for an efficient "in-line" intramolecular reaction.²⁴ They can polarize the P centers to enhance attack by nucleophile, and this effect must also be coupled with the effect of negative charge neutralization on the phosphate derivatives. Finally, the metal ions bound to the phosphorus

(20) ^{31}P NMR experiments have been conducted in 1 M OH^- and compared with those carried out in 0.1 M OH^- in order to investigate the origin of this phenomenon. However, apart from the expected changes in the relative ratios of the phosphate-containing products of the reaction, the two sets of spectra were identical. No new products that could be attributed to a pathway operative only at very high pH were observed.

(21) Olaghan, B. M.; House, D. A. *Inorg. Chem.* **1978**, *17*, 2197.

(22) Extrapolated from data of: Kirby, A. J.; Jencks, W. P. *J. Am. Chem. Soc.* **1965**, *87*, 3209.

(23) Hendry, P.; Sargeson, A. M. *J. Chem. Soc., Chem. Commun.* **1984**, 164.

(24) Knowles, J. R. *Annu. Rev. Biochem.* **1980**, *49*, 877.

oxygen atoms may also assist P-O bond rupture as a leaving group effect. For E. coli alkaline phosphatase therefore it is conceivable that two Zn²⁺ ions are bound to the phosphate ester and/or to the intermediate phosphorylated enzyme in order to assist their hydrolysis.

Acknowledgment. We are grateful to K. Barrow and G. Grossman of the Biochemistry Department, University of New South Wales, D. Fenn, and M. Whittaker of A.N.U. for their assistance with ³¹P spectroscopy and to the Microanalytical Unit A.N.U. for analyses and molecular weight determinations.

Decomposition and Ligand Substitution Reaction Mechanisms for Organometallic Radicals

Kenneth M. Doxsee, Robert H. Grubbs,* and Fred C. Anson

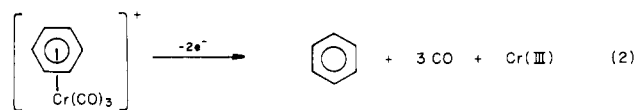
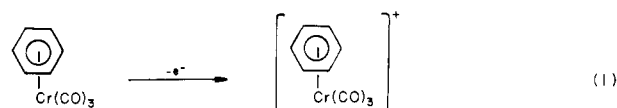
Contribution No. 6907 from the Laboratories of Chemistry, California Institute of Technology, Pasadena, California 91125. Received October 7, 1983

Abstract: The electrochemical oxidation of a series of (arene)chromium and (arene)tungsten tricarbonyl complexes has been examined. Studies regarding the oxidatively promoted decomposition of the chromium complexes are reported. Extension of these studies to the tungsten analogues has led to the observation of metal coordination sphere expansion upon one-electron oxidation, an observation of fundamental significance with regards to recent reports of dramatic reaction rate enhancements in odd-electron organometallic systems. The relationship of coordination sphere expansion to these and other problems of current mechanistic organometallic chemical interest, including the oxidative instability of (arene)chromium tricarbonyl complexes, is discussed.

Introduction

The participation of odd-electron intermediates in "traditional" organometallic reactions has become a matter of growing speculation and concern.¹⁻⁷ Recent reports on the electrocatalysis of ligand substitution⁸⁻¹⁰ and migratory insertion^{6,11} reactions and on the substitution lability of stable organometallic radicals^{12,13} clearly demonstrate the important role such radicals may play in organometallic reaction mechanisms. As part of an investigation of the reactivity of cationic metal carbonyl complexes with nucleophiles,¹⁴ we have examined the electrochemical oxidation of a series of (arene)chromium tricarbonyl complexes and of a tungsten analogue. Though the oxidation chemistry of such chromium complexes has attracted considerable interest,¹⁵⁻¹⁹

mechanistic details of the complex chemistry observed are lacking. At the current level of understanding,¹⁵ initial one-electron oxidation of the chromium complex (eq 1) is followed by rapid loss of ligands and further oxidation (eq 2). The latter is presumably a multistep process of unknown mechanism. We report our observations on the one-electron oxidation chemistry of (arene)chromium tricarbonyl complexes as a contribution toward a fuller understanding of the mechanistic complexities of these systems.



(1) Lawrence, L. M.; Whitesides, G. M. *J. Am. Chem. Soc.* **1980**, *102*, 2493-2494.

(2) Ashby, E. C.; Bowers, J. R., Jr. *J. Am. Chem. Soc.* **1981**, *103*, 2242-2250.

(3) Okuhara, K. *J. Am. Chem. Soc.* **1980**, *102*, 244-252.

(4) Klingler, R. J.; Huffman, J. C.; Kochi, J. K. *J. Am. Chem. Soc.* **1980**, *102*, 208-216.

(5) Krusic, P. J.; San Filippo, J., Jr.; Hutchinson, B.; Hance, R. L.; Daniels, L. M. *J. Am. Chem. Soc.* **1981**, *103*, 2129-2131.

(6) Magnuson, R. H.; Zulu, S.; T'sai, W.-M.; Giering, W. P. *J. Am. Chem. Soc.* **1980**, *102*, 6887-6888.

(7) Kochi, J. K. "Organometallic Mechanisms and Catalysis"; Academic Press: New York, 1978.

(8) Darchen, A.; Mahe, C.; Patin, H. *J. Chem. Soc., Chem. Commun.* **1982**, 243-245.

(9) Hershberger, J. W.; Kochi, J. K. *J. Chem. Soc., Chem. Commun.* **1982**, 212-214.

(10) Hershberger, J. W.; Klingler, R. J.; Kochi, J. K. *J. Am. Chem. Soc.* **1982**, *104*, 3034-3135.

(11) Magnuson, R. H.; Meirowitz, R.; Zulu, S.; Giering, W. P. *J. Am. Chem. Soc.* **1982**, *104*, 5790-5791.

(12) McCullen, S. B.; Walker, H. W.; Brown, T. L. *J. Am. Chem. Soc.* **1982**, *104*, 4007-4008.

(13) Shi, Q.-Z.; Richmond, T. G.; Troglor, W. C.; Basolo, F. J. *J. Am. Chem. Soc.* **1982**, *104*, 4032-4034.

(14) Doxsee, K. M.; Grubbs, R. H. *J. Am. Chem. Soc.* **1981**, *103*, 7696-7698.

(15) Degrand, C.; Radecki-Sudre, A.; Besancon, J. *Organometallics* **1982**, *1*, 1311-1315.

(16) Rieke, R. D.; Tucker, I.; Milligan, S. N.; Wright, D. R.; Willeford, B. R.; Radonovich, L. J.; Eyring, M. W. *Organometallics* **1982**, *1*, 938-950.

(17) Rieke, R. D.; Milligan, S. N.; Tucker, I.; Dowler, K. A.; Willeford, B. R. *J. Organomet. Chem.* **1981**, *218*, C25-C30.

(18) Llyod, M. K.; McCleverty, J. A.; Connor, J. A.; Jones, E. M. *J. Chem. Soc., Dalton Trans.* **1973**, 1768-1770.

(19) Gubin, S. P.; Khandkarova, V. S. *J. Organomet. Chem.* **1970**, *22*, 449-460.